

Review

Recent Progress of Hydrogenation and Hydrogenolysis Catalysts Derived from Layered Double Hydroxides

Zhihui Wang¹, Wei Zhang¹, Cuiqing Li^{2,*} and Chen Zhang^{2,*} 

¹ School of New Materials and Chemical Engineering, Beijing Institute of Petrochemical Technology, Beijing 102617, China

² Beijing Key Laboratory of Enze Biomass Fine Chemicals, Beijing Institute of Petrochemical Technology, Beijing 102617, China

* Correspondence: licuiqing@bipt.edu.cn (C.L.); zhangc@bipt.edu.cn (C.Z.)

Abstract: Layered double hydroxides (LDHs), also known as hydrotalcite-like compounds, are widely used in many fields due to their unique structural advantages. Based on LDHs, a wide range of metal catalysts could be synthesized with high metal dispersion, tunable acid-base properties, facile but flexible preparation methods, strong metal-support interaction, and thermal stability. Owing to these outstanding advantages, LDH-derived materials manifest great potential as catalysts, particularly in hydrogenation and hydrogenolysis reactions. More than 200 papers published in the past five years in this field clearly indicated the rapid development of these materials. In this respect, it is imperative and essential to provide a timely review to summarize the current progress and motivate greater research effort on hydrogenation and hydrogenolysis catalysts derived from LDHs. In this review, the applications of LDH-derived materials as heterogeneous catalysts in various hydrogenation and hydrogenolysis reactions were comprehensively discussed. Hydrogenation of unsaturated chemical bonds, hydrodeoxygenation of oxygenated compounds, hydrogenolysis of carbon–carbon bonds and hydrogenation of nitrites and nitriles were described. This review demonstrates the extraordinary potentials of LDH-derived catalysts in hydrogenation and hydrogenolysis reactions, and it is undoubted that LDH-derived catalysts will play an even more significant role in the foreseeable future.

Keywords: layered double hydroxides; hydrotalcite; hydrogenation; hydrogenolysis; catalysis



Citation: Wang, Z.; Zhang, W.; Li, C.; Zhang, C. Recent Progress of Hydrogenation and Hydrogenolysis Catalysts Derived from Layered Double Hydroxides. *Catalysts* **2022**, *12*, 1484. <https://doi.org/10.3390/catal12111484>

Academic Editor: Vladimir Sobolev

Received: 21 October 2022

Accepted: 17 November 2022

Published: 20 November 2022

Publisher's Note: MDPI stays neutral with regard to jurisdictional claims in published maps and institutional affiliations.



Copyright: © 2022 by the authors. Licensee MDPI, Basel, Switzerland. This article is an open access article distributed under the terms and conditions of the Creative Commons Attribution (CC BY) license (<https://creativecommons.org/licenses/by/4.0/>).

1. Introduction

Hydrogenation is one of the most fundamental processes in the chemical industry with diverse applications. In hydrogenation, atomic hydrogen is added to unsaturated chemical bonds in the presence of homogeneous or heterogeneous catalysts. Hydrogenolysis is another important type of reaction where a carbon–carbon bond or carbon–heteroatom bond is cleaved by hydrogen. In the past century, hydrogenation and hydrogenolysis are particularly important in the petrochemical industry to saturate alkenes or aromatics, remove sulfur or nitrogen atoms, increase fuel stability and decrease toxicity [1]. Recently, hydrogenation and hydrogenolysis attracted extensive attention for new objectives. Biomass utilization [2,3] and CO₂ hydrogenation [4,5], which are crucial processes for a sustainable human society, also heavily rely on the technological development of hydrogenation and hydrogenolysis. Using renewable H₂ produced from eco-friendly processes [6,7], hydrogenation and hydrogenolysis in biomass upgrade and CO₂ hydrogenation could greatly reduce the dependency on fossil fuels. In most industrial cases, hydrogenation or hydrogenolysis are catalyzed by supported metal catalysts based on transition metals such as Ni, Cu, Pd, or Pt [2,8,9].

Layered double hydroxides (LDHs) are layered inorganic materials consisting of positively charged brucite Mg(OH)₂-like layers and interlayer charge-compensating anions, as

shown in Figure 1 [10]. A typical type of LDHs is hydrotalcite (HT), a natural mineral with chemical composition of $\text{Mg}_6\text{Al}_2(\text{OH})_{16}\text{CO}_3 \cdot 4\text{H}_2\text{O}$ [11]. LDHs and natural hydrotalcite share similar structure, in which metal cations can be replaced by divalent and trivalent metal ions with similar atomic radii in the same crystal, and interlayer anions can be replaced by other intercalating anions. LDHs, also called hydrotalcite-like compounds, could be expressed with the general formula $[\text{M}^{2+}_{(1-x)}\text{M}^{3+}_x(\text{OH})_2]^{x+} \cdot [(\text{A}^{n-})_{x/n} \cdot z\text{H}_2\text{O}]^{x-}$ [12]. Common M^{2+} ions include Mg^{2+} , Cu^{2+} , Zn^{2+} and Ce^{2+} , while common M^{3+} include Al^{3+} , Fe^{3+} , and Cr^{3+} . These cations can be atomically and uniformly dispersed in the hydrotalcite layer. The formed cation layers lack interlayer interaction and have a negative net charge, which must be balanced by the inserted anions, and water molecules might also enter the interlayer region [13]. Interlayer anions are exchangeable, such as CO_3^{2-} , NO_3^- , SO_4^{2-} , Cl^- , F^- , acetate and salicylate. The x value in the general formula represents the molar ratio of $\text{M}^{2+}/(\text{M}^{2+} + \text{M}^{3+})$, and the range of its value has great influence on the composition and structure of hydrotalcite materials [10]. Both the magnitude of the charge density on the laminate and the extent to which the homocrystalline substitution of metal cations occurs depend on the x value, and a genuine LDH phase is usually found only at $0.2 < x < 0.4$ [14,15].

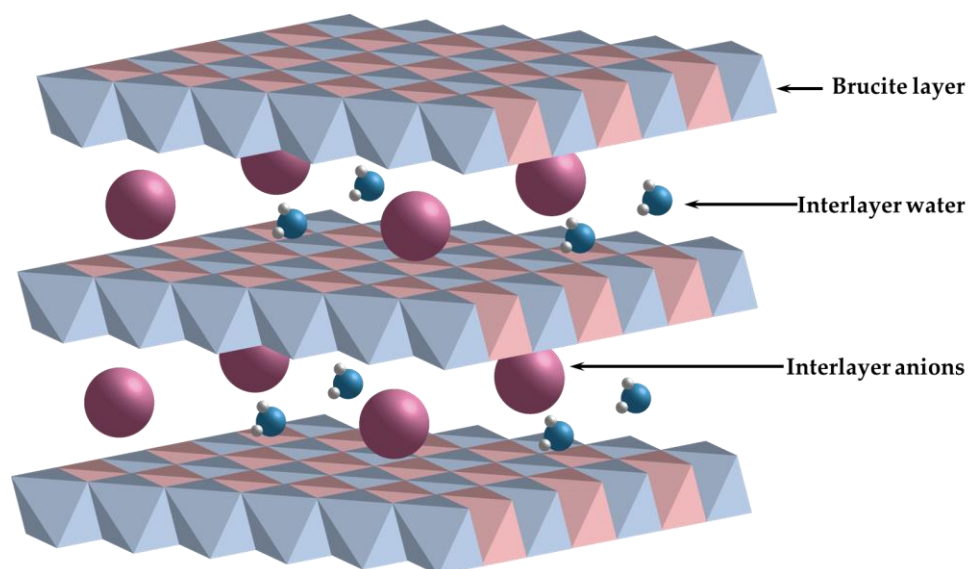


Figure 1. A Schematic illustration of LDH structure.

The unique structure, tunability of the layer and interlayer element composition, delamination property, structural topological transformations, and the confinement effect of LDHs provide LDH-derived materials great application potentials in many fields [14,16]. In heterogeneous catalysis, LDH can be applied as catalyst itself, catalyst support or catalyst precursor in many reactions such as C-C coupling, *N*-arylation, oxidation, hydrogenation, hydrogenolysis, etc. Although several review articles on catalytic applications of LDHs have been published [12,17–21], reviews focusing on hydrogenation and hydrogenolysis are still scarce to the best of the authors' knowledge. Furthermore, in the past few years, a large number of research articles on hydrogenation and hydrogenolysis over LDH-derived catalysts were published, demonstrating the significant development in the field. Therefore, we believe it is timely to provide a comprehensive and in-depth summary on the latest progress of LDH-derived catalysts for hydrogenation and hydrogenolysis. This review will focus on the applications of LDH-derived materials as hydrogenation and hydrogenolysis catalysts, highlighting physiochemical properties, structural properties and reactivity advantages of LDH-derived catalysts. Thermocatalytic processes catalyzed by heterogeneous catalysts will be the emphasis of this review, while electrocatalytic or photocatalytic research will not be discussed due to their distinct nature in mechanisms.

2. Type of LDH-Derived Catalysts for Hydrogenation and Hydrogenolysis

Generally, three types of LDH-derived catalysts are prepared and investigated: LDH-supported catalysts, LDH-derived mixed metal oxides (MMOs), and LDH-derived intermetallic compounds (IMCs). Table 1 shows several examples of different types of LDH-derived catalysts and their reported physiochemical properties. It could be noticed in the table that high specific surface area and small particle size could be readily achieved with catalysts from LDHs. This section will describe in detail the general advantages and synthesis protocols of these three types of LDH-derived materials.

Table 1. Examples of LDH-derived catalysts prepared with different methods.

Catalyst	Preparation Method	Surface Area (m ² /g)	Particle Size (nm)	Other Properties	Ref.
PdAg/ZnTi-LDH	Coprecipitation and photochemical reduction	131	5	Pore volume 2.63 cm ³ ·g ⁻¹ ; mean pore size 80.3 nm	[22]
Pt/CoAl-MMO	Coprecipitation and reduction–deposition	87	4–5	Pore volume 0.29 cm ³ ·g ⁻¹ ; mean pore diameter 3.83 nm	[23]
CuMgAl-MMO	Urea hydrolysis	213	–	Pore volume 0.95 cm ³ ·g ⁻¹	[24]
CuCoAl-MMO	Coprecipitation	92.9	3.1	Pore volume 0.69 cm ³ ·g ⁻¹	[25]
NiMoAl-MMO	Coprecipitation and ion exchange	93	4.6	Pore volume 0.13 cm ³ ·g ⁻¹ ; total acid sites 2.077 mmol·g ⁻¹	[26]
NiIn-IMC	Co-precipitation	126.4	5.8	–	[27]
NiMo-IMC	In situ co-reduction	189.2	18.6	–	[28]

2.1. LDH-Supported Catalysts

Because heterogeneous catalysts for hydrogenation and hydrogenolysis usually require the participation of metallic sites, pristine LDHs could not be used directly as hydrogenation and hydrogenolysis catalysts. Nevertheless, LDHs act as perfect support materials due to intrinsic structural superiorities. High specific surface area, hierarchical pore structure, abundant surface defects, strong metal-support interaction, surface acid-base sites with tunable strength or concentration, or inherent confinement effects have been reported for LDHs [14,20].

Major synthesis methods of LDHs include coprecipitation [29], urea hydrolysis, hydrothermal synthesis [30] and the sol-gel method [15]. Different synthesis methods directly affect the physical and chemical properties of the obtained LDH materials [31–33]. The most facile and common method is coprecipitation. By coprecipitation, crystallinity, particle size distribution, and stability of LDHs can be precisely controlled by adjusting the synthesis parameters such as pH, temperature, aging time, mixing rate, cation ratio and solution concentration [31,32]. Coprecipitation can be combined with the anion exchange method to modulate the structure and function of LDH-based materials by inserting ions or molecules between layers while keeping the basic structure unchanged, modifying the physiochemical properties or the surface properties of the material.

2.2. LDH-Derived Mixed Metal Oxide Catalysts

Mixed metal oxides (MMOs), which could be synthesized by the heat treatment of LDHs, showed high catalytic performance and received broad attention in hydrogenation and hydrogenolysis. LDH-derived MMOs inherit LDH characteristics such as controlled composition, high specific surface area, and uniform morphology. In addition, by converting metal hydroxides into metal oxides, highly dispersed metal oxides particles were generated, which could act as acid or base sites. The nature, intensity and concentration of these acid/base sites on MMOs could be tuned by controlling the type and molar ratio of metal cations in the precursors, preparation method, calcination temperature and

type of interlayer anions [20,34,35]. The high surface area and tunable acid/base property, as well as other advantages, make LDH-derived MMOs an ideal catalyst support material compared to the conventional metal oxide support. MMOs could also be used independently as hydrogenation/hydrogenolysis catalysts. For MMOs with hydrogenation-active metals such as Ni or Cu, the reduction of MMOs could generate highly dispersed metallic sites in situ which are catalytically active for hydrogenation/hydrogenolysis. Compared with supported metal catalysts prepared by impregnation, reduced MMOs as hydrogenation/hydrogenolysis catalysts are often more reactive, due to the high metal dispersion, abundant acid/base sites and strong metal–support interaction, as shown later in this review.

The calcination of LDHs to generate MMOs is a topological transformation process. During thermal transformation three temperature domains of LDH structure changes can be observed. The first structural change at around 190 °C corresponds to the dehydration of loosely bonded interlayer water, accompanied by the decrease in the layer spacing, while the layered structure is retained [36]. The second temperature domain in the range of 200–400 °C indicated dehydroxylation and the collapse of the layered structure of LDHs, in situ forming highly dispersed metal oxides [37]. The third domain in the range of 500–1000 °C is ascribed to the formation of sintered metal particles and spinel phases [36,38]. The structure and function of MMOs can be controlled by changing the topological transformation parameters such as heating rate, calcination temperature and calcination atmosphere of LDH precursors during the thermal treatment, leading to the modification of the catalytic performance of MMOs [10,17,34,39,40].

2.3. Intermetallic Compound Catalysts

Intermetallic compounds (IMCs), also called ordered alloy, is a special type of alloy composed of two (or more) metal elements with specific crystal structure and atomic composition. IMCs can be expressed as A_xB_y , where x and y are small integers, usually 1, 2 and 3 [41,42]. Compared with conventional alloys, IMCs exhibit completely or partially ordered surface structure. Figure 2 showed the structure of NiSb and NiBi IMCs catalysts prepared by Wei's group [43]. It could be noticed that high metal dispersion and uniform alloy composition were obtained with IMCs, which were important for catalytic reactivity. Due to the unique electronic and geometric properties, IMCs promote the activated adsorption of substrate molecules with specific patterns or configurations, thus achieving improved catalyst activity, selectivity and stability [41,44,45].

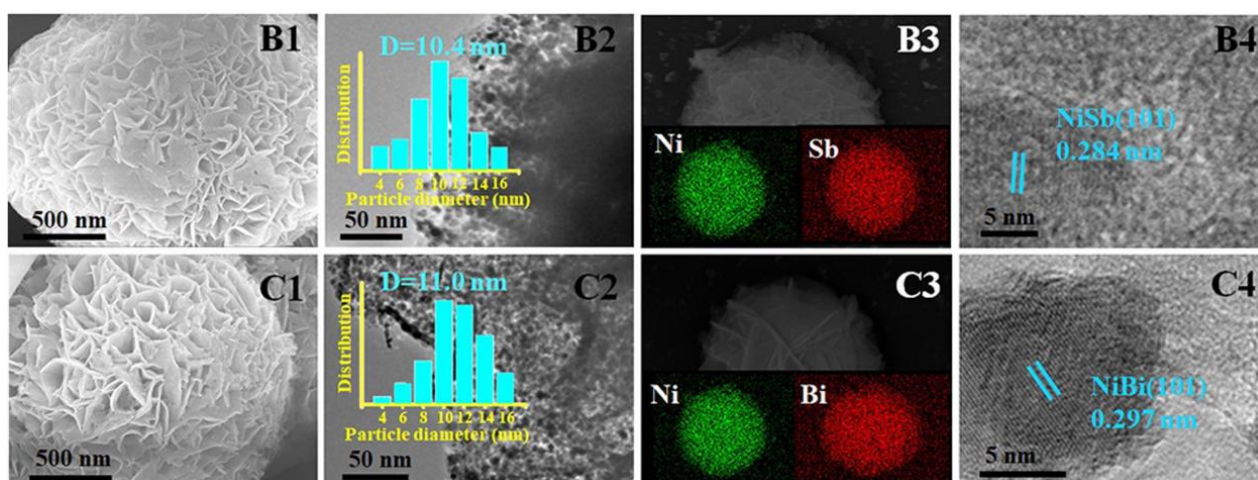


Figure 2. (B1) SEM, (B2) TEM and particle size distribution, (B3) elemental mapping, and (B4) lattice spacing images of NiSb IMC; (C1) SEM, (C2) TEM and particle size distribution, (C3) elemental mapping, and (C4) lattice spacing images of NiBi IMC [43]. (Copyright 2020, Elsevier).

The preparation of IMCs can be categorized into three methods, controlled colloid synthesis, inorganic capsule synthesis, and layered double hydroxide synthesis [42]. The synthetic method based on LDHs has particular advantages. The composition flexibility of LDH precursors enable the possibility of synthesizing a variety of IMC catalysts [45,46]. Metal elements of LDH layers have a high degree of dispersion at the atomic level, which is conducive to the formation of metal catalysts with high metal dispersion after the calcination-reduction process. The preparation of IMC nanocrystals using LDH precursors can be achieved by two methods, endogenous method or exogenous method. For the endogenous method, two metal components of IMCs (e.g., Ni, Co, Cu, Ga) are introduced simultaneously into the host layer of LDHs, followed by the calcination and reduction of LDH precursors, affording IMC catalysts. For noble metal elements (Au, Rh, Pd, Ir, Pt, etc.) or heavy metal elements (Sb, Sn, Bi, Pb, etc.) which are difficult or impossible to introduce into the LDH layer, the exogenous method can be adopted, in which noble metal or heavy metal salts are mixed with LDH precursors by impregnation, followed by calcination and reduction to obtain IMC catalysts.

3. Hydrogenation of Carbon-Oxygen Unsaturated Bonds

3.1. Hydrogenation of Ketones and Aldehydes

The hydrogenation of carbonyl groups in ketones and aldehydes to form hydroxy groups is an important process particularly in synthetic chemistry. This section will review research work on ketone or aldehyde hydrogenation catalyzed by LDH-derived catalysts. The selective hydrogenation of α - β unsaturated aldehydes including crotonaldehyde, citral and cinnamaldehyde will also be discussed. The hydrogenation of furfural, a highly important furan aldehyde derived from hemicellulose, will be reviewed in the next section separately.

For hydrogenation over heterogeneous catalysts, metal dispersion is crucial because high dispersion would naturally mean more active sites for reactions to take place. Non-precious metal catalysts such as Ni, Cu and Co could be synthesized by the calcination of corresponding LDH precursors prepared by coprecipitation. Because M^{2+} and M^{3+} ions are uniformly distributed in the brucite layers, the calcination of LDHs could in situ generate highly dispersed metal particles and more catalytic active sites for hydrogenation. For instance, Dragoi's group have shown that a reduced CuMgAl catalyst synthesized from LDH precursors exhibited particle sizes of 2.6 to 6.5 nm and high activity in cinnamaldehyde hydrogenation to cinnamyl alcohol [40]. Another study using CuMgAl-MMO of 1.4 to 2.4 nm metal particle size for benzyl aldehyde hydrogenation, obtained 85–93% selectivity of benzyl alcohol [47].

As shown in Table 2, precious metals are particularly effective in selective hydrogenation of unsaturated aldehydes. For precious metal catalysts such as Pt, Pd or Ru, using LDHs or LDH-derived MMOs as support could also generate catalysts with high precious metal dispersion. Many examples were found in the literature reporting metal particle sizes less than 5 nm using the conventional impregnation method on LDHs/MMOs owing to the abundant surface basicity to anchor metal species [48], such as Ru/MgAl-HT [49], Pd/MgAl-MMO [50] and Au/MgAl-MMO [51] for aldehyde/ketone hydrogenation. Notably, due to the special interlayer galleries of LDHs, an alternative way to load metals to the support other than impregnation is by intercalating metal-containing anions in LDHs by the ion exchange method. With this method, researchers were able to obtain a Pt/MgAl-HT catalyst with an average diameter of Pt nanoparticle being only 1.9 nm using $PtCl_6^{2-}$ [52]. Generally, as the catalyst particle size decreases, the number of low coordination sites such as the edges and corners of the metal increases, providing more active sites for the reaction and thus enhancing the catalytic activity of the catalyst [23,27,53].

Table 2. Catalytic performances of LDH-derived catalysts for hydrogenation of ketones and aldehydes.

Catalyst	Substrate	Reaction Conditions	Conversion (%)	Product Selectivity (%)	Ref.
Pt/ZnSnAl/C	2-Pentenal	80 °C; 3.0 MPa H ₂	28.5	2-Pentenol, 92.0	[54]
Cu/MgAl-HT	Benzaldehyde	250 °C	68	Benzyl alcohol, 93	[47]
Ru/MgAl-HT	Benzaldehyde	100 °C; 3.5 MPa H ₂	>63	Cyclohexanemethanol, 91.9	[49]
Au/Mg ₂ AlO	Crotonaldehyde	120 °C; 0.93 MPa H ₂	23.6	Crotyl alcohol, 62	[51]
Pt/MgAl-LDH	Cinnamaldehyde	80 °C; 2 MPa H ₂	92.6	Cinnamyl alcohol, 75.5	[52]
Pt/CoAl-MMO	Cinnamaldehyde	70 °C; 2 MPa H ₂	99.7	Cinnamyl alcohol, 72.5	[23]
Au/ZnAl	Cinnamaldehyde	130 °C; 1.5 MPa H ₂	100	Cinnamyl alcohol, 95.7	[53]
Pt/MgAl-LDH	Cinnamaldehyde	60 °C; 1 MPa H ₂	79.7	Cinnamyl alcohol, 85.4	[55]
PtGa/MgAlGa	Cinnamaldehyde	70 °C; 3 MPa H ₂	52.8	Cinnamyl alcohol, 70.7	[56]
Ir/MgAlFe	Cinnamaldehyde	60 °C; 3 MPa H ₂	94.4	Cinnamyl alcohol, 79.1	[57]
Pt/CoAl-LDH	Cinnamaldehyde	70 °C; 3 MPa H ₂	94.3	Cinnamyl alcohol, 91.9	[58]
CoGa-IMC	Cinnamaldehyde	100 °C; 2 MPa H ₂	100	Cinnamyl alcohol, 96	[59]
NiZnAl/C	Citral	140 °C; 1 MPa H ₂	100	Citronellol, 92.3	[60]
CoSn-IMC	Citral	160 °C; 4.0 MPa H ₂	100	Citronellol, 67.6	[61]
CuZnAl-MMO	Citral	80 °C; 1.0 MPa H ₂	99.8	Allylic alcohol, 75.1	[62]
NiBi-IMC	Unsaturated aldehydes	100 °C; 2 MPa H ₂	>90	Unsaturated alcohol, >93.2	[43]
NiIn-IMC	Unsaturated aldehydes	120–145 °C; 3 MPa H ₂	>56	Unsaturated alcohol, >44	[27]
Pt/MgCoAl	Unsaturated aldehydes	80 °C; 2 MPa H ₂	>87	Unsaturated alcohol, >80	[63]

Because metal particle size plays an important role in the reactivity of the catalyst, particularly for the selective hydrogenation of α - β unsaturated aldehydes, several methods were developed for tuning particle size in LDH-related catalysts. Xiang et al. prepared HT-supported Pt nanocrystal catalysts for the selective hydrogenation of cinnamaldehyde [55]. It is noticed in this research that the selectivity of cinnamyl alcohol was closely related to Pt particle size, while the size of the Pt nanocrystals could be finely tuned by controlling the amount of surfactant added. Another study provides an example of using different alcohols including ethylene glycol, methanol and ethanol for the reduction of Pt on MgAl-LDHs, generating different sizes of reduced Pt particles with distinct reactivity in cinnamaldehyde hydrogenation [64].

For LDH-derived catalysts, the fact that active metal particles were incorporated in the LDH or MMO matrix indicates strong metal-support interaction (SMSI) [65]. SMSI is a specific interaction effect between the support and the metal nanoparticles (NP). This interaction may lead to metal-metal bonding or the formation of intermetallic compounds in the catalyst [66], enhancing the stability of the metal particles in the catalyst. In addition, the topological transformation from LDHs to MMOs can be exploited to create SMSI by stabilizing the active metal particles in the oxide matrix, to prevent leaching and agglomeration [67–69]. Wang et al. reported a slight increase in particle size from 1.2 nm to 1.6 nm for the Pt catalyst supported on ZnSnAl-MMOs after 12 h of 2-pentenal hydrogenation reaction [54]. Metal-support interaction could also electronically and geometrically affect metal atoms, shifting the product distribution in selective hydrogenation [56,57,67]. For instance, the addition of ZnO into NiZnAl-MMOs could deactivate C=C adsorption on Ni sites, inducing increased citronellol selectivity in citral hydrogenation [60]. Oxygen vacancies, which play important roles in carbonyl hydrogenation, could also be readily generated by SMSI. Miao et al. reported the formation of oxygen vacancies at the metal-support interface of Pd/MgAl-LDHs [70] and Pt/CoAl-LDHs [58]. It is found that these oxygen vacancies are activation sites for C=O bonds, and significantly enhance the selectivity toward C=O hydrogenation over C=C bond hydrogenation. Although SMSI is important for catalysts, its actual mechanism on product selectivity is still complex and case-dependent. It is proposed in a study that SMSI could enhance the C=C bond adsorption on Pd sites on MgAl-LDHs, leading to an increased selectivity toward citronellal in citral hydrogenation [71], while another research on cinnamaldehyde hydrogenation over Pt/CoMgAl suggested that SMSI strengthened the carbonyl adsorption and inhibited C=C hydrogenation [63].

Wei's groups synthesized a series of intermetallic compound (IMC) catalysts using LDH precursors, including CoGa, CoIn, NiBi, CoSn and NiIn, for selective hydrogenation of unsaturated aldehydes [43,59,61]. It could be concluded from their research that by forming IMC catalysts, the electron density of active metal (Ni or Co) was modified due to electron transfer, leading to a change in adsorption conformation or adsorption strength which eventually affected product selectivity. The promising results from IMCs, as well as the convenient preparation method using LDH precursors, suggest a promising prospect of IMCs in heterogeneous catalysis.

For α - β unsaturated aldehydes, total hydrogenation of both C=C bonds and C=O bonds will also decrease yields toward desired products, and in most cases selective hydrogenation is pursued rather than total hydrogenation. The tunable acid–base properties of LDHs or MMOs play an important role in product distribution of selective hydrogenation of α - β unsaturated aldehydes [72,73]. It is shown that CuZnAl-MMO catalysts with the most Lewis acid sites which adsorbed citral molecules via the carbonyl group showed the highest selectivity toward allylic alcohol products such as geraniol and nerol [62]. Another study on Pt/MgAl-MMO also suggested that catalysts with stronger acidity were more prone to unsaturated alcohol production [74]. It is deduced that Lewis acid sites, such as metal cations, are adsorption and activation sites for C=O bond, and thus the selectivity of C=O bond hydrogenation products is closely associated with Lewis acidity of catalysts. LDH-derived catalysts often exhibit a close vicinity to Lewis acid sites for carbonyl adsorption and metal sites for hydrogenation, inducing synergistic effects for efficient hydrogenation of carbonyl bond in aldehyde or ketone hydrogenation [75].

3.2. Hydrogenation of Furfural

Furfural (FAL) is an important biomass platform chemical bridging biomass feedstock and bio-derived chemicals with an annual production exceeding 652 kilotons [76]. FAL could be converted from lignocellulose and their chemical versatility implies plentiful potential applications in the production of renewable C₅ chemicals [77]. C=C double bond and C=O double bond in furfural molecules require selective hydrogenation capability from catalysts to yield desired products. The most prevalent product derived from furfural is furfuryl alcohol (FOL), as more than 65% of FAL produced worldwide was converted into FOL [78]. The hydrogenation of FAL to yield furfuryl alcohol (FOL) could be achieved by various metals [77]. Non-precious metal Cu- and Ni-based catalysts prepared from LDH precursors were studied for carbonyl group hydrogenation to produce furfuryl alcohol, such as CuAl [79,80], CuCr [81,82], NiAl [83,84], NiSn [85], and CuNiAl [86,87]. Advantages of preparing Cu or Ni catalysts from LDH precursors are the small metal particle size and high stability, due to the uniform atom distribution in LDH precursors. Yang et al. reported the NiSn intermetallic compound catalyst prepared from LDH precursors exhibited a monometallic Ni particle with a size of around 10 nm. The high dispersion and the electronic modification effect of Sn resulted in a 99% selectivity toward FOL from FAL at 100 °C and 2 MPa, and a high stability after more than 30 h [85].

Considering that the C=O bond from the furfural molecule could interact with the basic site on the catalyst surface, metal catalysts with surface basicity were synthesized, with Mg being the most commonly used metal due to the facile preparation from MgAl-hydrotalcite. NiMgAl-MMOs synthesized by calcining hydrotalcite precursors displayed high reactivity for the hydrogenation of FAL to FOL, with the synergistic effect between metallic Ni species to dissociate H₂ and surface basic sites generated by Mg introduction to activate furfural via carbonyl groups [88]. Villaverde et al. prepared CuMgAl catalysts derived from HT-like phases possessed high copper dispersion as well as strong interactions between metallic copper and magnesium–aluminum support, resulting in better activity, selectivity and stability than impregnated Cu catalysts [89,90]. Since CuNiAl, NiMgAl, and CuMgAl all showed outstanding reactivity in furfural hydrogenation, it is reasonable that CuNiMgAl would also display desirable catalytic properties [91,92], and it is demonstrated that the

uniform distribution of highly dispersed CuNi particles and surface basicity were crucial for the enhanced catalytic performances [93].

3.3. Hydrogenation of Levulinic Acid

Levulinic acid (LA) is an important biomass platform chemical which can be produced by the acid-catalyzed hydrolysis of lignocellulose [94]. One of the most important downstream chemicals from LA is gamma-valerolactone (GVL), a stable and nontoxic lactone that has broad applications and could be further converted into valuable compounds [95]. For example, GVL could be transformed into 1,4-pentanediol (1,4-PDO) by a hydrogenative ring-opening reaction, and 1,4-PDO could go through an intermolecular dehydration to form 2-methyltetrahydrofuran (2MTHF) [26,96]. Two mechanisms for LA hydrogenation into GVL were proposed based on literature research. In the first mechanism [97], LA was initially hydrogenated to form 4-hydroxypentanoic acid on metallic sites, followed by the lactonization to yield GVL at acid or basic sites. The second mechanism [98] started with an isomerization of LA to the enol form, followed by the lactonization to produce angelica lactone, and ends with hydrogenation to produce GVL. Some studies stated that the hydrogenation was the rate-determining step, while the lactonization reaction proceeded rapidly [99]. High hydrogen pressure (0.5–3 MPa) is usually necessary for high conversion of LA, so that the sufficient amount of dissolved hydrogen in solvent enables LA hydrogenation [100]. Many catalysts based on LDHs or MMOs were reported to be efficient for converting LA to GVL with high yields. Based on the published research, it seems that MMO catalysts based on Cu, Ni or Co showed comparably high selectivity toward GVL from LA. For example, CuAl-MMO [82], NiAl-MMO [101,102] and CoAl-MMO [103] catalysts were synthesized by different research groups and all showed comparably high selectivity (>85%) toward GVL. Analogously, CoMoAl [104], NiMgAl [101] and CuMgAl [105] catalysts synthesized by calcination of LDH precursors also showed dominant GVL production. Noble metal supported on LDH or MMO materials were also efficient for LA hydrogenation. Notably, MMOs-supported noble metal catalysts with a much lower reaction temperature (40–80 °C) were reported recently, compared to a reaction temperature of 140–260 °C used by most non-noble metal catalysts. Pt supported on MgAl-MMO demonstrated a nearly complete LA conversion into GVL at 40 °C and 50 bar [106], while Ru supported on MgAl-MMO or MgLa-MMO also showed a GVL selectivity higher than 99% at 80 °C and 5 bar [107].

Although high selectivity toward GVL from LA was achieved by many catalysts, a major concern in LA hydrogenation catalysts that should be dealt with is catalyst deactivation. Several mechanisms were proposed, including particle sintering, coke deposition, or metal leaching [108,109]. Because LA conversion into GVL produces water in lactonization, it is probable that MgO and Al₂O₃ may undergo phase transition in the hydrothermal environment, with brucite MgO or γ -Al₂O₃ transformed into periclase or boehmite, respectively, leading to undesired changes in pore structure and surface property [110–112]. Deactivation of LDH or MMO catalysts in LA hydrogenation was also observed and studied for its mechanisms. Hu's research reported Ni leaching in NiMgAl-MMO catalysts in LA hydrogenation, mainly due to the detrimental effect of water to Mg or Al leading to structure collapse [101]. Hussain et al. observed significant decreases of LA conversion in a time-on-stream study of MgAl-MMO. After characterization on spent catalysts, it is confirmed that in addition to the coke deposition on catalyst surface, the MgAl-MMO catalyst adsorbed water to regain the layered structure due to the memory effect, though this deactivation was largely reversible by calcination at 450 °C in air [113]. Considering the structure destruction during the reaction, metal particle sintering becomes inevitable, as observed with Cu/MgAl-MMO catalysts that Cu particles sized increased from 2 to 5.3 nm after LA hydrogenation at 260 °C [114]. Therefore, the stability of LDH or MMO catalysts for LA hydrogenation is an unavoidable issue before the commercialization of the catalytic process.

3.4. Catalytic Hydrogenation of Monosaccharides

The conversion of biomass feedstocks to fuels or chemicals is an important approach to generate renewable energy resources. Lignocellulose depolymerization or fermentation could produce monosaccharides or sugar alcohols, which could be further transformed to various types of chemicals [115]. For example, cellulose or hemicellulose could be hydrolyzed into C₅ and C₆ sugar alcohols such as glucose, xylose, and arabinose. These sugar alcohols were listed by the US Department of Energy among the top 12 sugar-derived building block chemicals, which are stable and versatile to upgrade to commodity chemicals [116]. Yamaguchi et al. prepared hydrotalcite supported nickel phosphide with high activity and stability for the hydrogenation of glucose [117], xylose [118], and maltose [119] under mild condition. The authors indicated that the hydrotalcite support activated the carbonyl group of the saccharide molecules and donated electrons to Ni, while molecular hydrogen was activated by unsaturated Ni sites from Ni₂P. Another study on sugar hydrogenation using a physical mixture of PtSn/Al₂O₃ and MgAl-MMO proposed that the addition of MgAl-MMO could provide an alkaline environment in the reaction system to facilitate ring opening reactions of sugar molecules [120], which is a key step for carbonyl hydrogenation [121]. While supported LDH catalysts showed synergistic effects between support and active metal, LDH-derived MMOs were also active in sugar hydrogenation. Wu et al. have shown that reduced CuNiAl and CuNiAlM (M = Mg, Co, Cr and Fe) catalysts were effective for the hydrogenation of glucose and fructose into sorbitol and mannitol [122,123]. Pérez-Ramírez et al. also reported HT-derived CuNiAl catalysts could catalyze transfer hydrogenation of these sugars to the corresponding polyols [124]. In both research, characterization results indicated that metallic Cu and Ni were formed in the reduced catalysts, which could act as active sites for hydrogenation.

4. Hydrogenation of Carbon-Carbon Unsaturated Bonds

4.1. Partial Hydrogenation of Alkynes

The production of ethylene in oil refinery is often accompanied with acetylene as the byproduct. Because acetylene could poison Ziegler–Natta catalysts and significantly deteriorate the quality of polyethylene, a partial hydrogenation process is needed to eliminate ethylene and not overhydrogenate ethylene to ethane [125]. Acetylene hydrogenation is considered to be a structure-sensitive reaction in which catalyst composition plays a vital role in product selectivity [126]. Ma et al. obtained a Pd/MgAl-LDHs/Al₂O₃ catalyst by in situ synthesis of Pd/MgAl-LDHs on spherical Al₂O₃ surface, and another Pd/MgO-Al₂O₃ catalyst by calcination and reduction of synthesized Pd/MgAl-LDHs/Al₂O₃ [127]. The results indicated that both catalysts had larger surface area, lower surface acidity, uniform Pd particle size, and strong metal-support interaction, leading to higher catalytic activity and selectivity than impregnated Pd/Al₂O₃ [128]. The high dispersion of Pd on the HT surface is presumably originated from the acidic sites on the support surface which weakened the electron density of Pd, favored the formation of low-coordinated Pd sites and enhanced dispersion [129,130]. Because Ag could effectively inhibit the formation of coke and improve the activity and stability of the catalyst [125], PdAg bimetallic catalysts supported on LDH-derived MMOs were also studied for acetylene hydrogenation. Research on PdAg supported on LDH-derived ZnO-Al₂O₃ found that compared with Al₂O₃, ZnO-Al₂O₃-MMO could significantly inhibit the overhydrogenation of acetylene and decrease oligomer formation [131]. Research on PdAg supported by NiTi-MMOs for acetylene hydrogenation found that a large number of Ti³⁺ defective sites existed on the NiTi support, acting as active centers to activate hydrogen and increasing the electron density Pd, thus promoting the desorption of ethylene and improving reaction selectivity [132]. When switching NiTi to MgTi as the PdAg support, the electronic effect between Ti³⁺ and Pd was still present, combined with the acid–base property of the MgTi support, contributing to nearly 100% conversion and 83.8% selectivity to ethylene at 70 °C [133].

In addition to being used as a catalyst support, LDH materials after calcination and reduction can also be used directly as acetylene hydrogenation catalysts. Rives et al. [134,135]

prepared a series of NiZnAlCr hydrotalcite-like catalysts for the selective hydrogenation of acetylene. The introduction of Cr inhibited the formation of coke, while the addition of Zn enhanced the metal–support interaction and improved the dispersion of Ni. Liu et al. [136] prepared CuNiMgAl nanoalloy catalysts for acetylene partial hydrogenation using LDHs as the precursor. High metal dispersion and structural homogeneity of NiCu nanocrystals were observed, and this LDH-derived CuNiMgAl showed better selectivity, anti-coking ability and stability than the CuNi/MgAl-HT catalysts prepared by the impregnation method. The addition of iron in Cu-based MMOs could further improve selectivity and reduce oligomerization, because iron served as a structural promoter to disperse active metals [137]. Moreover, in another research investigating Cu/Fe_yMgO_x-type catalysts derived from LDHs, iron is proposed to facilitate the formation of bifunctional interfacial active site Cu^{δ-}Fe_{0.16}^{δ+}MgO_x, which is effective in activating acetylene and hydrogen and promoting the desorption of ethylene [138].

Similar to acetylene partial hydrogenation, the partial hydrogenation of phenylacetylene to styrene for the elimination of phenylacetylene is an important pretreatment step in styrene polymerization process. Several LDH-based catalysts have shown excellent performance in this reaction. Pd/HT catalysts were synthesized for the phenylacetylene hydrogenation, and it is proposed that the layered structure of HT may impose steric restriction on reactants, making Pd/HT more stereoselective in the product than the conventional supported Pd catalysts [139]. Duan's group presented a novel series of nickel phosphide catalysts from LDH precursors with high selectivity toward styrene. It is claimed that phosphorus incorporation increased the Ni–Ni bond length and decreased Ni electron density, leading to the desorption of styrene so that further hydrogenation was avoided [140].

4.2. Hydrogenation of Aromatic Ring

Aromatic compounds in transportation fuels are responsible for reduced cetane number and increased particulate emission, as well as potential health hazard accompanied by the emission [141–143]. Strict legislative restrictions on aromatic content all over the world encourage research efforts on aromatic rings hydrogenation as an effective strategy to eliminate aromatic compounds in fuels [144]. The urgent need for lignin upgrade in recent years also inspires research on efficient aromatic hydrogenation [145]. Bai et al. investigated the hydrogenation of phenol over a series of Ni-based MMO catalysts and over 90% selectivity of cyclohexanol was obtained at 110–150 °C [146–148]. It is pointed out that the strong metal–support interaction of MMO catalysts induced high metal dispersion and prevented agglomeration or sintering. Strong metal–support interaction was also important in aromatic hydrogenation over Pd supported by MMOs [149]. Highly dispersed Pd particles were formed on CoCeAl-MMO surface with a particle size smaller than 4 nm, providing plentiful active sites for H₂ dissociative adsorption and ring hydrogenation. The addition of Ce generated abundant oxygen vacancies, which activated phenol by forming phenoxy and accelerated the hydrogenation reaction. Reaction temperature and pressure also significantly affected hydrogenation activity, as relatively high temperature and high pressure were more preferable for benzyl ring hydrogenation products [150,151].

5. Hydrogenolysis of Oxygenated Compounds

5.1. Hydrogenolysis of Esters

Ester hydrogenation and hydrogenolysis are important reactions with particular interest in biomass upgrade. Esters, including fatty acid esters, lactones, and levulinic esters, could be either directly extracted or chemically converted from biomass feedstock. Because esters themselves have limited uses in the chemical industry, hydrodeoxygenation or hydrogenolysis is usually necessary to convert esters into valuable commodities such as alcohols or alkanes. Triacylglycerols from non-edible plant oils or animal fats could be converted into fatty acid esters by transesterification reactions. Due to their high oxygen content and low heating value as fuels [152], researchers attempted to upgrade fatty acid esters to diesel-range hydrocarbon (C₁₅–C₁₈) by hydrodeoxygenation. Cao et al. utilized

LDH-derived NiCuAl catalysts for the hydrogenolysis of soybean and waste cooking oils, and more than 80% yield for diesel-range hydrocarbons was obtained at 260 °C and 3 MPa of H₂ [153]. Lewis acid sites (Al³⁺) was thought to be active sites for decarbonylation by interacting with the oxygen atom and cleaving acyl C-O bond. Another study [154] using NiGaMgAl to catalyze the hydrodeoxygenation of methyl laurate (C₁₁H₂₃COOCH₃) also present a 99% yield toward C₁₁+C₁₂ hydrocarbons at 400 °C and 3 MPa. The promotional effect of Ga to Ni suppressed the C-C bond hydrogenolysis, accounting for the high hydrocarbon yield.

Converting esters to diols which could be used as monomers for polyester materials is another attractive tactic with practical needs. Ethylene glycol, an important monomer in the polymer industry, could be produced by an indirect pathway from syngas via dimethyl oxalate. Wei's group prepared CuZrMgAl-MMO catalysts for dimethyl oxalate hydrogenation and obtained 99.5% yield of ethylene glycol under 180 °C and 2 MPa [155]. According to in situ characterization techniques, the authors attributed the high reactivity to the Cu-O-Zr metal-support interfacial sites, where carbon-oxygen bonds were activated at Zr-related oxygen vacancies and hydrogenated at adjacent Cu sites. Li's group demonstrated that 1,4-pentanediol could be produced from bio-derived ethyl levulinate by hydrodeoxygenation over CuCoAl-MMO catalysts, where Lewis acid sites such as electrophile Cu⁺ or electron-deficient CoO_x were considered to be crucial for carbonyl adsorption and activation [25].

5.2. Hydrodeoxygenation of Lignin Derivatives

Lignin is a cross-linked three-dimensional amorphous polymer composed of aromatic units, accounting for 10–35 wt.% in lignocellulosic material [145,156]. The rapid development of the biomass industry cogenerated more than 100 million tons of lignin annually [157]. Various aromatic chemicals could be produced by lignin valorization, yet only a small portion of lignin was actually utilized for chemical production. Lignin depolymerization is a complex and challenging task, with the pivotal issue being the cleavage of C-C bond and C-O bond. Hydrogenolysis is an effective way to break C-O linkage, and various LDH-derived catalysts were demonstrated to be highly reactive for lignin hydrogenolysis due to its high metal dispersion and adjustable acid-base properties. Flower-like Ni₂P-Al₂O₃ catalysts were obtained by reduction of red phosphorus with NiAl-LDH precursors at 500 °C by Li's group [158]. Ni₂P-Al₂O₃ showed high alkane selectivity in hydrogenolysis of poplar lignin oil. The high reactivity was attributed to the high exposure of cantilevered conical Ni sites with strong C-O bond break capability and plentiful acid sites to activate the substrate and H₂, as shown in Figure 3. Other research stated that acid sites, especially Lewis acid sites, facilitated deoxygenation of lignin derivatives by adsorbing the electron-rich phenyl ring or oxygen atoms, promoting ring hydrogenation or deoxygenation of methoxy or carbonyl [159,160]. Oxygen vacancies are also important for constructing high reactivity LDH-derived catalysts for lignin hydrogenolysis. Reducible oxide such as CoO_x [161] or CeO_x [162] in MMO catalysts could form surface oxygen vacancies to adsorb or activate oxygen-containing functional groups, greatly benefiting lignin deoxygenation reaction.

Among the common linkages that exist in lignin, the most recurring linkage is the β-O-4 linkage, constituting 50% of all linkages [145]. Therefore, model compounds with β-O-4 linkages were often synthesized to investigate catalyst reactivity in lignin depolymerization [163–165]. Wang et al. prepared a NiMgAl-C composite catalyst using lignosulfonate as the carbon precursor to impose electronic modifications to Ni [164]. The synthesized catalysts showed promising results in terms of conversion and selectivity in hydrogenolysis of model compounds and real lignin. The lamellar structure of LDHs could also be utilized to improve catalytic performance. Beckham and colleagues presented an inspiring study, where HT-derived catalysts with intercalated nitrates produced phenol monomers 2–3 times more than catalysts without nitrates in hydrogenolysis of model compounds [166]. It is proposed that intercalated nitrates not only increased accessibility to

basic active sites but also directly participated in the hydrogenolysis process, as the activity could be recovered after the nitrate reservoir was depleted and replenished.

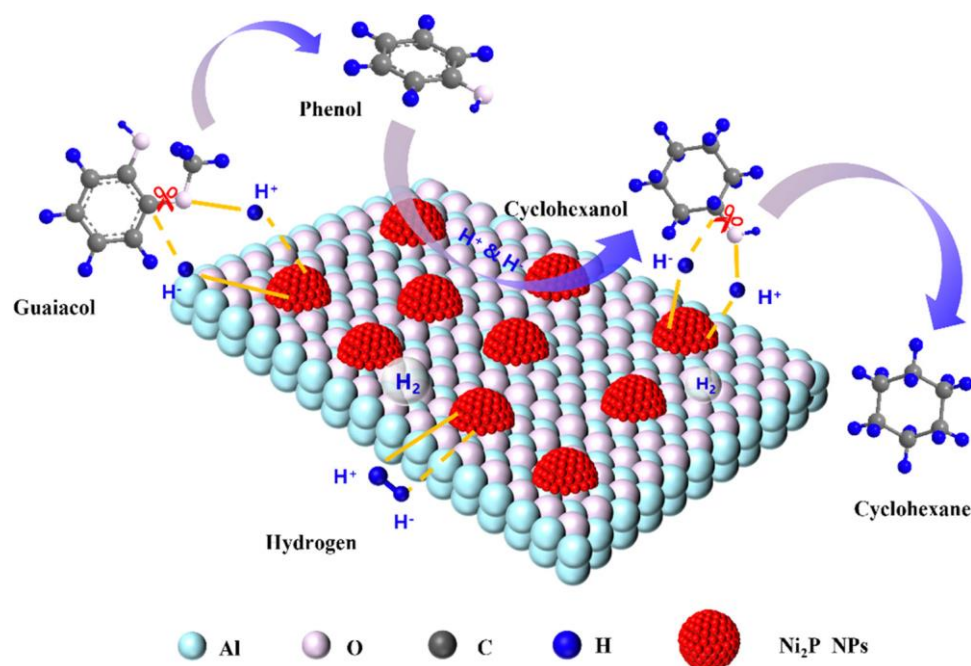


Figure 3. Reaction mechanism of guaiacol hydrodeoxygenation over NiP catalysts [158]. (Copyright 2022, American Chemical Society).

5.3. Hydrodeoxygenation of Furfural

C₅ polyols are important types of chemicals with huge demands in the polymer industry. Such polyols are traditionally produced from petroleum resources. Recently, researchers have developed the catalytic transformation of furfural to various polyols via hydrodeoxygenation. For furfural conversion to pentanediols (PDO), although early in 1930s Adkins and Connor presented Cu-Cr catalysts to convert furfuryl alcohol to pentanediols [167], MMO catalysts for catalytic conversion of furfurals to pentanediols were extensively studied in the last decade. Initially, Pt supported on CoAl-MMO [168] or MgAl-HT [169] synthesized by two separate research groups showed high reactivity in furfural hydrogenolysis toward 1,5-pentanediol and 1,2-pentanediol, respectively, at 110–140 °C and 1.5–3 MPa. The role of these supports is related to the basicity which might change adsorption preference leading to ring-opening reactions. Subsequently, Huang's group noticed that CuMgAl-MMO [170] or CuAl-MMO [171] alone could also catalyze the formation of pentanediols at a relatively high pressure of 6 MPa. The distinct difference in reactivity and selectivity between conventional impregnated Cu/Al₂O₃ catalyst and coprecipitated CuAl-MMO catalyst demonstrated the advantage of the much smaller Cu particle size of the MMO catalyst (1.9 nm) compared to the impregnated catalyst (16.7 nm) [171]. Another advantage of MMO catalysts is the partially reduced metal species on the surface, as several studies presented positive correlations between partially reduced metal species and pentanediol selectivity [24,172,173]. Based on published literature, the mechanism of furfural conversion to pentanediols could be summarized, as shown in Figure 4. Furfural is first hydrogenated to produce furfuryl alcohol, and then furfuryl alcohol will go through C-O bond scission to afford 1,2-pentanediol or 1,5-pentanediol depending on the catalyst property. Acid–base active sites [24,174–177] or partially reduced metal species [172,173] are proposed to influence the adsorption configuration of furfuryl alcohol, resulting in the activation of different C-O bond and different pentanediol products.

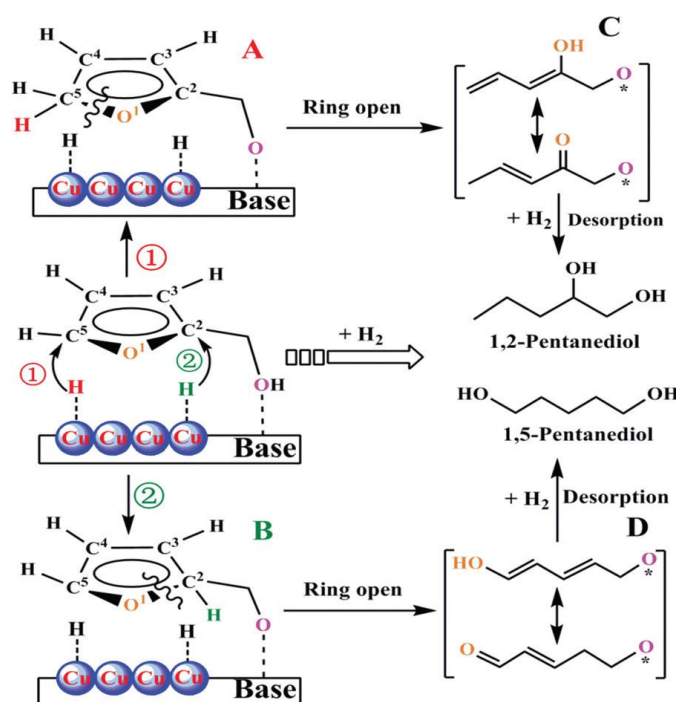


Figure 4. Reaction mechanism of furfural hydrogenolysis over CuMgAl-*MMO* catalysts [170]. (Copyright 2022, Royal Society of Chemistry).

5.4. 5-Hydroxymethylfurfural Hydrodeoxygenation

Cellulose could be transformed into 5-hydroxymethylfurfural (HMF), a platform chemical with various downstream products [77]. Many important compounds can be produced from HMF. For example, 2,5-dimethylfuran (DMF) by HMF hydrodeoxygenation could be used as fuel additive due to its high-octane number and energy density [178,179]. HMF could also be converted to 2,5-furandimethanol (FDM) [180,181] via hydrogenation of carbonyl group, to 2,5-tetrahydrofurandimethanol (THFDM) [180,182] via furan ring hydrogenation of FDM, or to 2,5-dimethyltetrahydrofuran (DMTHF) [183–185] via furan ring hydrogenation of DMF. FDM and THFDM could be used as building blocks in polymer synthesis, and DMTHF is a potential fuel additive [77]. As shown in Table 3, the selectivity toward DMF, FDM, or DMTHF could be controlled by choosing adequate reaction conditions or metal catalysts [180,184].

Table 3. Catalytic performances of LDH-derived catalysts for 5-hydroxymethylfurfural hydrodeoxygenation¹.

Catalyst	Reaction Condition	Conversion (%)	Major Product Selectivity (%)	Ref.
NiAl- <i>MMO</i>	80 °C; 2 MPa H ₂	96.0	THFDM, 74	[180]
Ru/MgAl-HT	220 °C; 1 MPa H ₂	100.0	DMF, 58	[181]
NiAl- <i>MMO</i>	180 °C; 1.2 MPa H ₂	100.0	DMTHF, 97.4	[182]
Ni-Cu/HT	90 °C; 1 MPa H ₂	99	DMF, 67	[185]
CoZnAl- <i>MMO</i>	130 °C; 0.7 MPa H ₂	>99.9	DMF, 74.2	[186]
CuCoNiAl- <i>MMO</i>	180 °C; 1 MPa H ₂	99.8	DMF, 95.3	[187]
CuZnAl- <i>MMO</i>	180 °C; 1.2 MPa H ₂	100	DMF, 90.1	[188]
Co-N-C/NiAl- <i>MMO</i>	170 °C; 1.5 MPa H ₂	99.9	DMF, 100	[189]
NiZnAl	100 °C; 1.5 MPa H ₂	100	FDM, 98.2	[190]
Cu@Co/CoAlO _x	180 °C; 1.2 MPa H ₂	100	DHTMF, 83.6	[191]
CuCoCe- <i>MMO</i>	210 °C; 1.5 MPa H ₂	100	DMF, 96.5	[192]
NiCoAl- <i>MMO</i>	120 °C; 4 MPa H ₂	100	1,2,6-HTO, 64.5	[193]
Cu _{1.5} Mg _{1.5} Al	150 °C, 6 MPa H ₂	100	1,2-HDO, 40	[194]

¹. THFDM, 2,5-tetrahydrofurandimethanol; FDM, 2,5-furandimethanol; DMF, 2,5-dimethylfuran; DMTHF, 2,5-dimethyltetrahydrofuran; 1,2,6-HTO, 1,2,6-hexanetriol; 1,2-HDO, 1,2-hexanediol.

The transformation of HMF to afford DMF could be accomplished by various metal catalysts. CuAl- [80], NiAl- [180,182], and CuNiAl-MMO [195] catalysts with high metal dispersion showed excellent performance for the conversion of HMF to DMF, with DMF yields higher than 90%. In contrast, CoAl showed relatively lower DMF selectivity [186,187], likely due to its lower hydrogenation reactivity [196]. The conversion of HMF into DMF requires multifunctional catalysts with dual active sites catalyzing C=O hydrogenation and C-O hydrogenolysis. Wang et al. [188] studied the HMF hydrodeoxygenation over CuZnAl-MMO catalysts, claiming that Cu^+ species acted as C-O cleavage sites and Cu^0 species acted as C=O adsorption sites. The synergy between Cu^+ and Cu^0 species promoted the selective transformation of multi-functional groups of HMF molecules, thus improving catalyst reactivity and selectivity. However, these active sites might be susceptible to deactivation caused by changes in the metal chemical state [189]. This issue could be tackled by the incorporation of Zn generating strong Cu-O-Zn interaction by charge compensation, stabilizing active Cu^+ species, influencing adsorption configuration and preventing Cu agglomeration [186,190]. In another study on LDH-derived CuCoAl catalysts, Wang et al. pointed out that interfacial sites played key roles in the formation of different reaction intermediates in the catalytic hydrodeoxygenation of HMF [191]. C=O bond in the reactant was hydrogenated by the oxygen vacancies from CoO_x site to form hydroxy groups, while C=C bond was hydrogenated by Cu-Co interface positions. A similar interfacial effect is observed in reduced CuCoCe [192] and CoMgFe [197] catalysts as well, where oxygen vacancies formed on CuCeO_x or CoFeO_x interface activated the C-O bond and promoted C-O cleavage.

The hydrogenolysis of HMF to hexanediols or hexanetriols over LDH-derived catalysts were also probed by researchers. NiCoAl-MMO [193] and Pt supported on MgAl-MMO [198] were effective in converting HMF to 1,2,6-hexanetriol at 120–160 °C and 3–4 MPa. A 64.5% yield was obtained with a 0.5Ni2.5CoAl catalyst at 120 °C and 4 MPa. 1,2-Hexanediol could be produced over CuMgAl-MMO catalysts at 150 °C and 4–6 MPa [194]. The structure–activity relation could be inferred by two correlations reported in Hu’s research [194], as shown in Figure 5: a positive correlation between basic sites and catalyst turnover frequency (TOF), and a negative correlation between Cu particle size and catalyst TOF. These observations hinted at the crucial role of Cu particle size and basicity, which controlled the catalysts reactivity and selectivity in HMF hydrogenolysis, analogous to furfural hydrogenolysis. Conceivably, HMF or its hydrodeoxygenated product 5-methyl furfuryl alcohol were adsorbed on active sites in a tilted mode with C-O bonds interacting with active sites, leading to the C-O bond cleavage to form polyols [193,199].

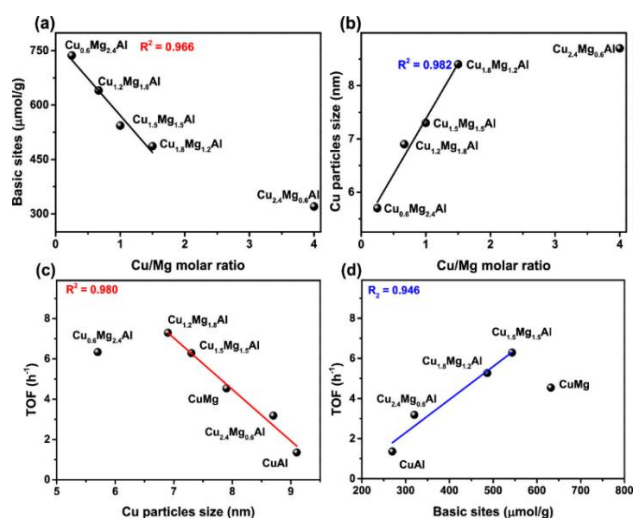


Figure 5. Influence of the molar ratio of Cu/Mg on the (a) distribution of basic sites and (b) Cu particle size. (c) Correlation between the Cu particle size and TOF value and (d) basic sites and TOF value [194]. (Copyright 2022, American Chemical Society).

6. CO₂ Hydrogenation

The chemical fixation of CO₂ into value-added products is a pivotal process in CO₂ utilization to reduce CO₂ emission, decrease fossil fuel usage, and alleviate the greenhouse effect. Numerous research on catalytic conversion of CO₂ were conducted in recent years, and exciting progress was made for the hydrogenation of CO₂ into various chemicals including methane, methanol, carbonates, carboxylic acid, etc. [200,201]. Compared to regular hydrogenation catalysts, unique advantages in adsorption capacity of LDH-derived catalysts for CO₂ hydrogenation are recognized to further promote catalyst performance through adsorption enhancement [202]. Because a number of reviews were published in the past few years regarding the broad CO₂ hydrogenation field [9,201,203,204] or specific CO₂ hydrogenation reaction [205], the goal of this review is to analyze the applications of LDH or MMO catalysts in CO₂ hydrogenation, focusing on CO₂ thermocatalytic conversion into methanol and methane.

6.1. CO₂ Conversion to Methanol

The CO₂ hydrogenation to methanol is a promising strategy for CO₂ utilization, as methanol is a key feedstock that can be industrially converted to a wide range of chemicals such as light olefins and gasoline [206,207]. For example, the methanol-to-olefin (MTO) process by Dalian Institute of Chemical Physics, China, has been commercialized with an annual production of 7.16 Mt per year by the end of 2018 [208]. Methanol could be produced from syngas (CO₂/CO/H₂) using an industrial Cu/ZnO/Al₂O₃ catalysts synthesized from zincian malachite, (Cu,Zn)₂(OH)₂CO₃, by the coprecipitation of metal nitrates (Cu, Zn and Al) [209]. It has been conclusively demonstrated that the superior reactivity of Cu/ZnO/Al₂O₃ stemmed from the structure defects of the Cu surface and the promotional effect of Zn to Cu [210]. Owing to the advantages of the MMO catalysts mentioned above, research efforts were devoted to preparing CuZnAl-based catalysts from LDH precursors aiming to obtain catalysts more reactive than the industrial Cu/ZnO/Al₂O₃ catalyst. Behrens and coworkers presented CuZnAl-MMO catalysts through the coprecipitation of nitrate solution at 25 °C and a constant pH value of 8 ± 0.7. The synthesized CuZnAl was intrinsically more active in CO₂ hydrogenation than the industrial CuZnAl catalyst when normalized by Cu surface area, due to the highly dispersed Cu particles (7 nm) and strong interfacial interaction between embedded Cu particles and ZnAl₂O₄ matrix [211].

To further improve the catalyst reactivity of CuZnAl catalysts, the addition of fourth metal elements was explored in CO₂ hydrogenation to methanol. A wide range of metals have been added to CuZnAl by coprecipitation of metal precursors, with different metals exhibiting different modification effects. The addition of zirconium to CuZnAl could increase the basicity, strengthen the adsorption of CO₂ and promote the formation of methanol [212,213]. Similar effects were observed for Mn, La, Ce and Y, as a series of CuZnAlX (X = Mn, La, Ce, Zr and Y) catalysts were synthesized in a study from Sun's group, and modified CuZnAlX catalysts showed a higher portion of strong basic sites, CO₂ conversion and methanol selectivity than the unmodified CuZnAl [214]. Yttrium modified CuZnAl possessed a higher surface area and more dispersed Cu particles, resulting in a higher methanol yield per gram of catalysts than the unmodified CuZnAl [215]. The addition of indium to CuZnAl increased the methanol selectivity by inhibiting CO formation, yet decreased TOF of methanol formation [216].

Modifications on synthesis procedures were also attempted to induce structural transformation of the CuZnAl-based MMO catalysts. Different alumina sources [217,218], Zn precursors [219,220], phase of precipitated precursors [221], atomic ratios [222–224], sequence of precursor addition [225,226], calcination temperature [227], precipitation pH [228] and precipitation agents [229] in synthesis procedures of MMO catalysts commonly resulted in diverse catalytic activity, selectivity or stability for CO₂ hydrogenation. These phenomena were often attributed to the difference in acid–base properties, exposed Cu surface area, particle size, phase composition, etc. However, due to the structural complexity of active sites in methanol synthesis [210,230], it is not easy to acquire a direct correlation

between catalyst physiochemical properties and catalytic performance. More in-depth research on catalyst structure, especially in situ characterizations, is essential to unveil the structure–activity relationship for CuZnAl catalysts.

For the industrial Cu/ZnO/Al₂O₃ catalyst, the role of alumina is considered to be a structural promoter that prevents Cu particles from aggregation [231]. Kühl et al. conducted experiments to partially replace Al with trivalent cations Cr and Ga [232]. The substitution of Al by Cr reduced the interaction between Cu and oxide matrix, causing Cu particle growth during CO₂ hydrogenation. In contrast, the substitution of Al by Ga turns out to be rather effective in improving catalyst activity, and this improvement was ascribed to the fact that Ga addition could stabilize Cu phase and benefit the catalytic activity of Cu particles. Other research presented consistent conclusions. CuZnGa-MMO catalysts showed higher Cu surface area and dispersion than CuZnAl using the aqueous miscible organic solvent treatment (AMOST) method, which involves an additional step of treating LDHs precipitates with an organic solvent [233,234].

6.2. CO₂ Conversion to Methane

The conversion of CO₂ to methane, namely CO₂ methanation, is also known as the Sabatier reaction first reported in 1897. In the current age of pursuing carbon neutrality, Sabatier reaction is experiencing its renaissance, as CO₂ methanation becomes a convenient strategy to convert CO₂ to a widely used energy resource in a sustainable manner. Two types of reaction mechanisms for CO₂ methanation were proposed. The first mechanism presumes the direct methanation of CO₂ to methane via formate, carbonate or bicarbonate, while the second mechanism requires the conversion of CO₂ to CO before CO is converted to CH₄ [235–237]. The actual mechanism may vary depending on the catalyst type, reaction temperature, etc. As CuZn-based catalysts constitute the majority of catalysts for methanol synthesis, Ni-based catalysts represent the most important category of CO₂ methanation catalysts [236]. Another important factor for the catalyst of methane formation is the amount and strength of basic sites [238,239]. In this respect, MMO catalysts derived from MgAl-LDHs were studied comprehensively due to its advantageous capability of combining tunable basic sites with dispersed metal particles.

The strong dependence of CO₂ conversion to catalyst basicity, especially medium strength basic sites, was reported by many researchers, as indicated by the positive correlation between medium strength basic sites and CO₂ conversion or TOF [240–242]. Basic sites, such as OH[−] and O^{2−}, could adsorb and activate CO₂ to form carbonate or bicarbonate species [243,244]. It is noticed that increased basicity was related to the increased amount of bicarbonate-like species for NiMgAl-MMO catalysts, while bicarbonate is the main CO₂ adsorption product and an important intermediate for methane formation at low temperatures [245]. It is also speculated that higher basicity promotes the hydrogenation rate of surface-adsorbed carbonates [246]. Moreover, medium strength basic sites promote monodentate carbonates formation, as monodentate is more readily hydrogenated to form CH₄ than bidentate carbonates [238,245]. The introduction of certain metal promoters is a facile way to manipulate MMO catalyst basicity. Metals including V [247], Y [240], Fe [246,248], Mn [242], Zr [249], Ce [250], La [251–253] and Cu [241] have been demonstrated to result in increased concentration of basic sites. Apart from changes in basicity, metal promoters could also adjust the metal–support interaction and increase Ni dispersion. Ho and colleagues [253] claimed that CO₂ interacted more strongly with NiLaAl than NiAl due to higher basicity and more dispersed Ni particles, leading to a much higher low-temperature activity in CO₂ methanation of NiLaAl. In situ characterization studies suggested that both dissociative activation (forming CO) and associative activation (forming bicarbonate and carbonate) of CO₂ were simultaneously observed for NiLaAl, while for NiAl, CO₂ was successively activated by the dissociative pathway and then associative.

Oxygen vacancies are also proposed as a crucial factor for CO₂ methanation, as shown in Figure 6 [250]. Oxygen vacancies could act as Lewis acid sites to interact with electron-rich oxygen atoms from CO₂ for CO₂ chemisorption and activation [254]. DFT calculations

confirmed that oxygen vacancies on simulated the NiCeAl surface contributed to the lower CO₂ adsorption energy than the NiAl surface [255]. Oxygen vacancies also facilitate the formation of active oxygen species, which could react with CO₂ to produce monodentate or bidentate carbonates, accelerating the methanation reaction [249,250]. He et al. confirmed that NiZrAl ternary MMO catalysts showed more oxygen vacancies and basic sites than NiAl binary counterpart.

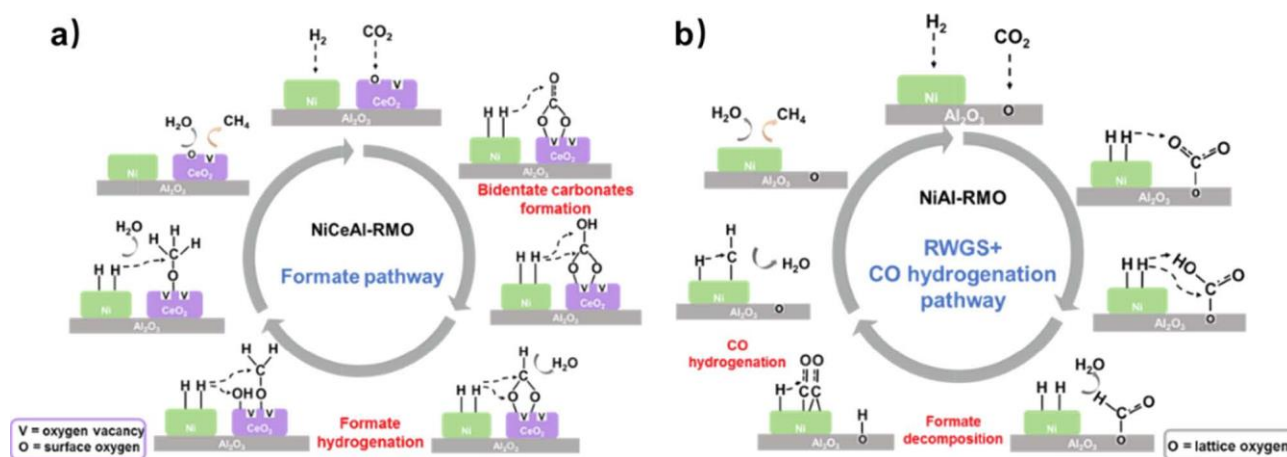


Figure 6. The role of oxygen vacancies in CO₂ methanation via (a) formate pathway and (b) CO pathway [250]. (Copyright 2022, Elsevier).

7. Hydrogenation in C-C Coupling Processes

In recent years, the demand for bio-derived fuels or chemicals stimulates extensive interests in converting biomass feedstock into various types of renewable fuels. Regarding the fact that most biomass platform chemicals consist of oxygen-containing functional groups such as hydroxy or carbonyl groups, C-C coupling or C-C bond formation via aldol condensation, dehydration/hydrodeoxygenation, and hydrogenation are effective strategies to produce downstream chemicals, especially in the synthesis of long chain hydrocarbons such as jet fuel in the range of C₈–C₁₆. Regarding the advantages of LDH-derived MMOs simultaneously possessing metallic, acidic and basic sites, they become ideal candidates either as catalyst supports or as the catalyst themselves to achieve the cascade hydroconversion of C-C coupling for biomass upgrade. In some cases [256–262], C-C coupling to produce chemicals was accomplished by a two-stage process, with the first stage aimed at aldol condensation and dehydration using HT or MMO catalysts, and the second stage aimed at hydrogenation using non-HT and non-MMO catalysts. These studies, which did not use HT or MMO as hydrogenation catalysts, will not be discussed in this review. The following section will examine literature work on HT- or MMO-catalyzed hydrogenation in the C-C coupling processes.

Acetone, an inexpensive byproduct in lignocellulose fermentation, could undergo aldol condensation with itself or other chemicals to produce products with longer chains. The transformation of acetone to methyl isobutyl ketone (MIBK), an important chemical with extensive applications, is a typical example of the multifunctionality of LDH-derived materials. MIBK could be converted from acetone via three consecutive steps: aldol condensation catalyzed by bases, dehydration catalyzed by acids, and hydrogenation catalyzed by metals [263]. Regarding the advantages of LDH-derived MMOs, they are catalytically active as supports (Pd on ZrCr [263], MgAl [264,265] and CoAl [266]) or catalysts themselves (NiMgAl [267] and CuAl [268]) to achieve the one-pot conversion of acetone to MIBK. Because the sequence of the three steps are crucial for MIBK production from acetone, the concentration and the strength of acidic, basic, and metallic sites are expected to be balanced in order to minimize side products [264]. In order to obtain the optimal catalysts, catalysts with different concentrations of acid or base sites were prepared and tested. According to experimental results, it is generally believed that excessively

high acidity or basicity would lead to over-condensation products and reduce MIBK yields [264,267].

Cyclopentanone (CPO, C₅H₈O), a bio-derived chemical produced by aqueous phase furfural rearrangement, could be transformed to jet-fuel range cycloalkanes by C-C coupling reactions. Cai and coworkers synthesized a bifunctional Ni/MgAl/active carbon catalyst using a MgAl-HT precursor in an integrated C-C coupling/hydrogenation process for the conversion of CPO with over 80% yield toward C₁₀ or C₁₅ alkanes [269,270]. The authors ascribed the remarkable performance to the enhanced strength of the basic sites of MgAl-MMO, promoting trimerization of CPO more effectively than conventional oxide support such as MgO, Al₂O₃, NaY or TiO₂, as well as the strong hydrodeoxygenation activity of Ni than Fe, Co or Cu. Another research combining MgAl-MMO with Pd in CPO trimerization also obtained high trimer yield [271]. In addition to CPO, C-C coupling of other ketones were also attempted to produce elongated alkanes using LDH or MMO catalysts. Sheng et al. performed MIBK self-condensation over Pd-modified MgAl-HT to produce dodecanol, with MgAl-HT support acting as a base catalyst for self-aldol condensation [272].

Alcohols could also be used for C-C coupling after dehydrogenation to form aldehydes or ketones, followed by aldol condensation, dehydration and hydrogenation. For these processes, metallic sites on MMO catalysts could catalyze the dehydrogenation of the initial alcohol and the hydrogenation of the unsaturated ketones, while acid–base sites catalyze condensation and dehydration reaction. A few alcohols were studied for their C-C coupling applications, including 2-hexanol [273], propanol [274], octanol [275] and ethanol [276,277]. It is commonly believed in these studies that numbers of metal, acid, and base sites should be delicately designed to prevent side reactions and by-products.

8. Hydrogenation of Nitrites and Nitriles

8.1. Hydrogenation of Organic Nitrites

The selective hydrogenation of aromatic nitro compounds to produce anilines is important in synthetic chemistry. The major challenges in this process are to selectively reduce nitro groups and not affect other functional groups. Various types of noble or non-noble metal catalysts were developed to achieve this goal [278]. For catalysts with noble metals such as Pd or Pt, key factors that determine their catalytic performance are metal dispersion and the resistance to particle agglomeration. LDHs or MMOs, which exhibit hierarchical structure able to immobilize active species, stand out as desirable catalyst support. Wang et al. showed that Pd supported on MgAl-LDHs demonstrated higher catalytic activity and selectivity than Pd/SiO₂ or Pd/C in substituted nitrobenzene hydrogenation, likely due to the confining effect of metallic Pd in layers of LDHs [279]. Similar conclusions were reached in another study studying Pd supported on MgAl-MMOs, MgO and γ -Al₂O₃ in nitrobenzene hydrogenation [48]. Results showed that Pd/MMOs were superior to the latter two in terms of turnover frequency and stability, and authors ascribed the superiority to the high dispersion of Pd particles on MMOs and the anchoring effect of MMOs to prevent Pd aggregation. Non-noble MMO catalysts such as CuZnAl also showed high activity in the hydrogenation of nitro groups [280]. The activity of CuZnAl was attributed to the Cu-ZnO_x active sites, similar to the one used in CO₂ conversion, as mentioned above.

A more challenging case in aromatic nitro compound hydrogenation is the selective hydrogenation of nitro groups when other readily reducible groups are presented, as in the case of nitrostyrene hydrogenation to yield vinylaniline. Corma and Serna have reported a breakthrough by using Au/TiO₂ and Au/Fe₂O₃ to hydrogenate 3-nitrostyrene to selectively produce 3-vinylaniline [281]. Recently, a series of gold catalysts supported on hydrotalcites also showed promising activity. Zhang's group discovered that thiolated Au₂₅ nanoclusters supported on calcined ZnAl-HT showed complete 3-nitrostyrene conversion in a wide temperature window from 90 to 135 °C with 3-vinylaniline selectivity higher than 98%. The high selectivity was attributed to the ZnAl-HT support adsorbing nitro groups rather than

vinyl groups [282]. Follow-up research comparing MgAl-, ZnAl-, and NiAl-HT as catalyst support observed that the amount of basic sites were in the order of MgAl > NiAl > ZnAl, while the 3-vinylaniline yield followed the order of MgAl < NiAl < ZnAl, suggesting that medium to weak basicity of the HT surface might benefit the reactivity [283]. Because nitro groups were generally believed to readily adsorb on basic surface, the role of calcined HT is speculated to be adsorption sites for nitro groups, in synergy with the gold particles which activate hydrogen. Nonetheless, the choice of HT support used for nitrostyrene hydrogenation catalysts still request special attention, as another research indicated that the selectivity toward vinyl hydrogenation could be enhanced by changing HT composition [284].

8.2. Hydrogenation of Nitriles

Hydrogenation of nitrile is an important industrial route for amines production. To inhibit byproducts such as secondary or tertiary imines, bases such as alkali bases or ammonia are commonly added along with metal catalysts [285]. The inherent basicity of MgAl-MMO materials makes them potential candidates for the hydrogenation of nitriles to produce amines. Tichit and coworkers prepared a series of Ni-containing catalysts based on LDH precursors for catalytic hydrogenation of nitriles. They discovered that the introduction of Mg in LDH precursors was effective in decreasing the surface acidity of the catalyst, decreasing the adsorption strength of primary amines, and thus preventing further coupling reaction between amines and imines. [286,287]. Cao et al. formulated a core-shell catalyst by coating nickel-based nanocomposites with LDHs or layered double oxides (LDOs), to catalyze the selective hydrogenation of benzonitrile to N-benzylaniline or benzylmethylaniline. It was found that the structural and acid-base properties of the LDH/LDO-coated nanocomposites could be switched by calcination or hydration according to the memory effect of LDHs [288]. Their following work on LDH-derived NiMgAl-MMO catalysts for the hydrogenation of benzonitrile also showed that the presence of strong metal-support interactions in NiMgAl catalysts could effectively inhibit the leaching or aggregation of Ni nanoparticles, accounting for the excellent stability of NiMgAl-MMO than the impregnated Ni/Mg_{0.75}Al_{0.25} catalysts [289]. The strong metal-support interaction was also observed in another study, in which a highly stable and active Co₂P supported on HT was prepared and studied for the ammonia-free selective hydrogenation of various nitriles to corresponding primary amines [290]. Compared to Al₂O₃, SiO₂, or carbon support, HT support stabilized Co species and prevented their oxidation, leading to enhanced reactivity and stability.

9. Future and Prospect of LDH-Derived Catalysts for Hydrogenation and Hydrogenolysis

Hydrogenation and hydrogenolysis are important reactions particularly in the petrochemical industry, biomass upgrade and CO₂ conversion. In the past decade, researchers have carried out extensive research on the application of LDH-derived catalysts in hydrogenation and hydrogenolysis. As reported in numerous studies mentioned above, superior reactivity of LDHs and their derived catalysts undoubtedly demonstrates outstanding advantages over conventional catalysts in the following aspects:

- (1) Various facile preparation methods, including co-precipitation, hydrothermal methods, ion exchange, urea hydrolysis, etc., could be used to prepare LDH-derived catalysts. These preparation methods are generally mature and well-established, facilitating the wide application and scale-up production of LDH materials.
- (2) The appropriate amount and strength of acidity/basicity are crucial for the design of multifunctional catalysts, and these properties could be achieved with LDH-derived materials. LDHs and MMOs possess high concentrations of acid/base sites, which are key sites for adsorption and reaction. For example, as discussed in this review, acidic sites could catalyze deoxygenation reactions, while basic sites could interact with carbonyl groups or catalyze aldol condensation. More importantly, the acid-base properties of LDHs and their derivative materials can be finely modulated by controlling the main layer element composition, interlayer ion species of the LDH precursor, and other synthesis parameters.

- (3) Metal particle size is crucial for the reactivity and selectivity of metal catalysts. In hydrogenation or hydrogenolysis reactions, metal catalysts with high metal dispersion will provide more active sites for dissociative activation of hydrogen and surface reaction to take place, resulting in increased reaction rates and decreased catalyst usages. For LDH-supported metal catalysts, hydroxy groups and interlayer galleries could promote the dispersion of metal particles. For MMO or IMC catalysts, because metal cations are uniformly distributed in the atomic level within LDH layers, the calcination of LDH precursors would generate MMOs with highly dispersed metal atoms. Therefore, LDH-derived materials become ideal catalysts for hydrogenation or hydrogenolysis due to their capability of generating small metal particles.
- (4) For MMO or IMC catalysts, when LDHs are calcined at high temperatures, active metal atoms are immobilized in the metal oxide matrix. This interaction between active metals and oxide matrix results in the formation of strong metal–support interactions (SMSI). SMSI is important not only in effectively preventing particle aggregation or sintering of the active metal during reaction but also modifying the electronic properties and catalytic reactivity of active metals.

Although much progress was made in the field of hydrogenation or hydrogenolysis catalysis over LDH materials, several challenges remained as follows:

- (1) The synthesis procedures of LDHs were studied thoroughly, but for LDH-derived catalysts more optimization and mechanism research on the preparation methods are still necessary. For example, for MMO catalysts, the relationship between preparation parameters (e.g., metal precursors, precipitation pH, crystallization time, calcination temperature, reduction temperature, etc.) and physiochemical properties is still vague or case-dependent.
- (2) The structure of LDH-derived catalysts is also currently unclear, which deserves more characterization efforts or theoretical predictions. The surface composition of LDH-derived catalysts, the electronic and geometric interactions between metal nanoparticles and neighboring components, and the origin of acidity/basicity of LDH-derived materials, are largely unknown, leading to difficulties in studying structure–reactivity relationships and catalyst design.
- (3) LDHs show a unique “memory effect” and good reversible topological conversion properties after heat treatment over a wide range of temperatures. Accordingly, how LDH-derived catalysts go through structure transformation during the reaction process also needs in-depth research. For biomass-related hydrogenation or hydrogenolysis research, this issue is important because water is often present either as reactant or product, which might lead to topological transformation of LDH derivatives. More research on structure transformation of LDH-derived catalysts before, during, or after reaction will be valuable for a broader application of LDH-derived catalysts.

10. Conclusions

In this review, the applications of LDH-derived materials in the field of catalytic hydrogenation and hydrogenolysis are comprehensively summarized. LDH-derived catalysts in hydrogenation and hydrogenolysis could be categorized into three types: LDH-supported catalysts, mixed metal oxides, and intermetallic compounds, while different types of catalysts exhibit different structure and physiochemical properties. The tunability in composition and property of these LDH-derived materials makes them versatile in many applications. As demonstrated by numerous examples mentioned above, LDH-derived catalysts showed superior reactivity owing to their unique advantages. Therefore, based on the current research progress, it could be envisaged that research on hydrogenation or hydrogenolysis over LDH-derived catalysts will keep on increasing rapidly in the future, and industrial applications of LDH-derived catalysts will also be expanding due to their desirable characteristics.

Author Contributions: Z.W.: Investigation, Writing—Original Draft, W.Z.: Validation, Supervision. C.L.: Writing—Review and Editing. C.Z.: Conceptualization, Writing—Review and Editing, Funding acquisition. All authors have read and agreed to the published version of the manuscript.

Funding: The authors would like to acknowledge funding support provided by National Natural Science Foundation of China (No. 21905027) and Beijing Education Committee Science and Technology Project (No. KM202010017007).

Conflicts of Interest: The authors declare no conflict of interest.

References

1. Ramachandran, R.; Menon, R.K. An overview of industrial uses of hydrogen. *Int. J. Hydrogen Energy* **1998**, *23*, 593–598. [[CrossRef](#)]
2. Corma, A.; Iborra, S.; Velty, A. Chemical routes for the transformation of biomass into chemicals. *Chem. Rev.* **2007**, *107*, 2411–2502. [[CrossRef](#)] [[PubMed](#)]
3. Gallezot, P. Conversion of biomass to selected chemical products. *Chem. Soc. Rev.* **2012**, *41*, 1538–1558. [[CrossRef](#)] [[PubMed](#)]
4. Wang, W.-H.; Himeda, Y.; Muckerman, J.T.; Manbeck, G.F.; Fujita, E. CO₂ hydrogenation to formate and methanol as an alternative to photo- and electrochemical CO₂ reduction. *Chem. Rev.* **2015**, *115*, 12936–12973. [[CrossRef](#)] [[PubMed](#)]
5. Wang, W.; Wang, S.; Ma, X.; Gong, J. Recent advances in catalytic hydrogenation of carbon dioxide. *Chem. Soc. Rev.* **2011**, *40*, 3703–3727. [[CrossRef](#)]
6. Qureshi, F.; Yusuf, M.; Kamyab, H.; Vo, D.-V.N.; Chelliapan, S.; Joo, S.-W.; Vasseghian, Y. Latest eco-friendly avenues on hydrogen production towards a circular bioeconomy: Currents challenges, innovative insights, and future perspectives. *Renew. Sustain. Energy Rev.* **2022**, *168*, 112916. [[CrossRef](#)]
7. Yusuf, M.; Farooqi, A.S.; Keong, L.K.; Hellgardt, K.; Abdullah, B. Contemporary trends in composite ni-based catalysts for CO₂ reforming of methane. *Chem. Eng. Sci.* **2021**, *229*, 116072. [[CrossRef](#)]
8. Ruppert, A.M.; Weinberg, K.; Palkovits, R. Hydrogenolysis goes bio: From carbohydrates and sugar alcohols to platform chemicals. *Angew. Chem. Int. Ed.* **2012**, *51*, 2564–2601. [[CrossRef](#)]
9. Yang, H.; Zhang, C.; Gao, P.; Wang, H.; Li, X.; Zhong, L.; Wei, W.; Sun, Y. A review of the catalytic hydrogenation of carbon dioxide into value-added hydrocarbons. *Catal. Sci. Technol.* **2017**, *7*, 4580–4598. [[CrossRef](#)]
10. Fan, G.; Li, F.; Evans, D.G.; Duan, X. Catalytic applications of layered double hydroxides: Recent advances and perspectives. *Chem. Soc. Rev.* **2014**, *43*, 7040–7066. [[CrossRef](#)]
11. Cavani, F.; Trifirò, F.; Vaccari, A. Hydrotalcite-type anionic clays: Preparation, properties and applications. *Catal. Today* **1991**, *11*, 173–301. [[CrossRef](#)]
12. Feng, J.; He, Y.; Liu, Y.; Du, Y.; Li, D. Supported catalysts based on layered double hydroxides for catalytic oxidation and hydrogenation: General functionality and promising application prospects. *Chem. Soc. Rev.* **2015**, *44*, 5291–5319. [[CrossRef](#)] [[PubMed](#)]
13. Yu, J.; Wang, Q.; O'Hare, D.; Sun, L. Preparation of two dimensional layered double hydroxide nanosheets and their applications. *Chem. Soc. Rev.* **2017**, *46*, 5950–5974. [[CrossRef](#)] [[PubMed](#)]
14. Wang, Q.; O'Hare, D. Recent advances in the synthesis and application of layered double hydroxide (ldh) nanosheets. *Chem. Rev.* **2012**, *112*, 4124–4155. [[CrossRef](#)]
15. Yan, K.; Wu, G.; Jin, W. Recent advances in the synthesis of layered, double-hydroxide-based materials and their applications in hydrogen and oxygen evolution. *Energy Technol.* **2016**, *4*, 354–368. [[CrossRef](#)]
16. Zhao, M.-Q.; Zhang, Q.; Huang, J.-Q.; Wei, F. Hierarchical nanocomposites derived from nanocarbons and layered double hydroxides—Properties, synthesis, and applications. *Adv. Funct. Mater.* **2012**, *22*, 675–694. [[CrossRef](#)]
17. Xu, Z.P.; Zhang, J.; Adebajo, M.O.; Zhang, H.; Zhou, C. Catalytic applications of layered double hydroxides and derivatives. *Appl. Clay Sci.* **2011**, *53*, 139–150. [[CrossRef](#)]
18. Takehira, K. Recent development of layered double hydroxide-derived catalysts—Rehydration, reconstitution, and supporting, aiming at commercial application—. *Appl. Clay Sci.* **2017**, *136*, 112–141. [[CrossRef](#)]
19. Zhang, F.; Xiang, X.; Li, F.; Duan, X. Layered double hydroxides as catalytic materials: Recent development. *Catal. Surv. Asia* **2008**, *12*, 253. [[CrossRef](#)]
20. Xu, M.; Wei, M. Layered double hydroxide-based catalysts: Recent advances in preparation, structure, and applications. *Adv. Funct. Mater.* **2018**, *28*, 1802943. [[CrossRef](#)]
21. Yan, K.; Liu, Y.; Lu, Y.; Chai, J.; Sun, L. Catalytic application of layered double hydroxide-derived catalysts for the conversion of biomass-derived molecules. *Catal. Sci. Technol.* **2017**, *7*, 1622–1645. [[CrossRef](#)]
22. Shen, Y.; Yin, K.; An, C.; Xiao, Z. Design of a difunctional Zn-Ti LDHs supported PdAu catalyst for selective hydrogenation of phenylacetylene. *Appl. Surf. Sci.* **2018**, *456*, 1–6. [[CrossRef](#)]
23. Tian, Z.; Li, Q.; Hou, J.; Pei, L.; Li, Y.; Ai, S. Platinum nanocrystals supported on coal mixed metal oxide nanosheets derived from layered double hydroxides as catalysts for selective hydrogenation of cinnamaldehyde. *J. Catal.* **2015**, *331*, 193–202. [[CrossRef](#)]
24. Fu, X.; Ren, X.; Shen, J.; Jiang, Y.; Wang, Y.; Orooji, Y.; Xu, W.; Liang, J. Synergistic catalytic hydrogenation of furfural to 1,2-pentanediol and 1,5-pentanediol with LDO derived from CuMgAl hydrotalcite. *Mol. Catal.* **2021**, *499*, 111298. [[CrossRef](#)]

25. Wu, J.; Gao, G.; Sun, P.; Long, X.; Li, F. Synergetic catalysis of bimetallic CuCo nanocomposites for selective hydrogenation of bioderived esters. *ACS Catal.* **2017**, *7*, 7890–7901. [\[CrossRef\]](#)
26. Zhang, G.; Li, W.; Fan, G.; Yang, L.; Li, F. Controlling product selectivity by surface defects over CuO-decorated Ni-based nanocatalysts for γ -valerolactone hydrogenolysis. *J. Catal.* **2019**, *379*, 100–111. [\[CrossRef\]](#)
27. Li, C.; Chen, Y.; Zhang, S.; Xu, S.; Zhou, J.; Wang, F.; Wei, M.; Evans, D.G.; Duan, X. Ni-in intermetallic nanocrystals as efficient catalysts toward unsaturated aldehydes hydrogenation. *Chem. Mater.* **2013**, *25*, 3888–3896. [\[CrossRef\]](#)
28. Liu, W.; Yang, Y.; Chen, L.; Xu, E.; Xu, J.; Hong, S.; Zhang, X.; Wei, M. Atomically-ordered active sites in NiMo intermetallic compound toward low-pressure hydrodeoxygenation of furfural. *Appl. Catal. B* **2021**, *282*, 119569. [\[CrossRef\]](#)
29. Wang, Y.; Chen, Z.; Zhang, M.; Liu, Y.; Luo, H.; Yan, K. Green fabrication of nickel-iron layered double hydroxides nanosheets efficient for the enhanced capacitive performance. *Green Energy Environ.* **2022**, *7*, 1053–1061. [\[CrossRef\]](#)
30. Liu, B.; Xu, S.; Zhang, M.; Li, X.; Decarolis, D.; Liu, Y.; Wang, Y.; Gibson, E.K.; Catlow, C.R.A.; Yan, K. Electrochemical upgrading of biomass-derived 5-hydroxymethylfurfural and furfural over oxygen vacancy-rich NiCo-layered double hydroxides nanosheets. *Green Chem.* **2021**, *23*, 4034–4043. [\[CrossRef\]](#)
31. Bukhtiyarova, M.V. A review on effect of synthesis conditions on the formation of layered double hydroxides. *J. Solid State Chem.* **2019**, *269*, 494–506. [\[CrossRef\]](#)
32. Theiss, F.L.; Ayoko, G.A.; Frost, R.L. Synthesis of layered double hydroxides containing Mg²⁺, Zn²⁺, Ca²⁺ and Al³⁺ layer cations by co-precipitation methods—A review. *Appl. Surf. Sci.* **2016**, *383*, 200–213. [\[CrossRef\]](#)
33. Othman, M.R.; Helwani, Z.; Martunus; Fernando, W.J.N. Synthetic hydrotalcites from different routes and their application as catalysts and gas adsorbents: A review. *Appl. Organomet. Chem.* **2009**, *23*, 335–346. [\[CrossRef\]](#)
34. Debecker, D.P.; Gaigneaux, E.M.; Busca, G. Exploring, tuning, and exploiting the basicity of hydrotalcites for applications in heterogeneous catalysis. *Chem.—Eur. J.* **2009**, *15*, 3920–3935. [\[CrossRef\]](#) [\[PubMed\]](#)
35. He, S.; An, Z.; Wei, M.; Evans, D.G.; Duan, X. Layered double hydroxide-based catalysts: Nanostructure design and catalytic performance. *Chem. Commun.* **2013**, *49*, 5912–5920. [\[CrossRef\]](#)
36. Yang, W.; Kim, Y.; Liu, P.K.T.; Sahimi, M.; Tsotsis, T.T. A study by in situ techniques of the thermal evolution of the structure of a Mg–Al–CO₃ layered double hydroxide. *Chem. Eng. Sci.* **2002**, *57*, 2945–2953. [\[CrossRef\]](#)
37. Zhao, X.; Zhang, F.; Xu, S.; Evans, D.G.; Duan, X. From layered double hydroxides to ZnO-based mixed metal oxides by thermal decomposition: Transformation mechanism and UV-blocking properties of the product. *Chem. Mater.* **2010**, *22*, 3933–3942. [\[CrossRef\]](#)
38. Kim, Y.; Yang, W.; Liu, P.K.T.; Sahimi, M.; Tsotsis, T.T. Thermal evolution of the structure of a Mg–Al–CO₃ layered double hydroxide: Sorption reversibility aspects. *Ind. Eng. Chem. Res.* **2004**, *43*, 4559–4570. [\[CrossRef\]](#)
39. Takehira, K.; Shishido, T. Preparation of supported metal catalysts starting from hydrotalcites as the precursors and their improvements by adopting “memory effect”. *Catal. Surv. Asia* **2007**, *11*, 1–30. [\[CrossRef\]](#)
40. Dragoi, B.; Ungureanu, A.; Chiriac, A.; Ciotonea, C.; Rudolf, C.; Royer, S.; Dumitriu, E. Structural and catalytic properties of mono- and bimetallic nickel–copper nanoparticles derived from MgNi(Cu)Al-LDHs under reductive conditions. *Appl. Catal. A* **2015**, *504*, 92–102. [\[CrossRef\]](#)
41. Armbrüster, M.; Schlögl, R.; Grin, Y. Intermetallic compounds in heterogeneous catalysis—A quickly developing field. *Sci. Technol. Adv. Mater.* **2014**, *15*, 034803. [\[CrossRef\]](#)
42. Yang, Y.; Wei, M. Intermetallic compound catalysts: Synthetic scheme, structure characterization and catalytic application. *J. Mater. Chem. A* **2020**, *8*, 2207–2221. [\[CrossRef\]](#)
43. Yu, J.; Yang, Y.; Chen, L.; Li, Z.; Liu, W.; Xu, E.; Zhang, Y.; Hong, S.; Zhang, X.; Wei, M. NiBi intermetallic compounds catalyst toward selective hydrogenation of unsaturated aldehydes. *Appl. Catal. B* **2020**, *277*, 119273. [\[CrossRef\]](#)
44. Furukawa, S.; Komatsu, T. Intermetallic compounds: Promising inorganic materials for well-structured and electronically modified reaction environments for efficient catalysis. *ACS Catal.* **2017**, *7*, 735–765. [\[CrossRef\]](#)
45. Marakatti, V.S.; Peter, S.C. Synthetically tuned electronic and geometrical properties of intermetallic compounds as effective heterogeneous catalysts. *Prog. Solid State Chem.* **2018**, *52*, 1–30. [\[CrossRef\]](#)
46. Zang, Y.; Wang, Y.; Gao, F.; Gu, J.; Qu, J. Highly active two-dimensional NiAl intermetallic compounds derived from Al-substituted layered double hydroxides for CO₂ hydrogenation reduction. *Fuel* **2021**, *299*, 120929. [\[CrossRef\]](#)
47. Jayesh, T.B.; Itika, K.; Ramesh Babu, G.V.; Rama Rao, K.S.; Keri, R.S.; Jadhav, A.H.; Nagaraja, B.M. Vapour phase selective hydrogenation of benzaldehyde to benzyl alcohol using Cu supported Mg–Al hydrotalcite catalyst. *Catal. Commun.* **2018**, *106*, 73–77. [\[CrossRef\]](#)
48. Sangeetha, P.; Shanthy, K.; Rao, K.S.R.; Viswanathan, B.; Selvam, P. Hydrogenation of nitrobenzene over palladium-supported catalysts—Effect of support. *Appl. Catal. A* **2009**, *353*, 160–165. [\[CrossRef\]](#)
49. Chaudhari, C.; Sato, K.; Miyahara, S.-i.; Yamamoto, T.; Toriyama, T.; Matsumura, S.; Kusuda, K.; Kitagawa, H.; Nagaoka, K. The effect of Ru precursor and support on the hydrogenation of aromatic aldehydes/ketones to alcohols. *ChemCatChem* **2022**, *14*, e202200241. [\[CrossRef\]](#)
50. Martínez-Ortiz, M.J.; de la Rosa-Guzmán, M.A.; Vargas-García, J.R.; Flores-Moreno, J.L.; Castillo, N.; Guzmán-Vargas, A.; Morandi, S.; Pérez-Gutiérrez, R.M. Selective hydrogenation of cinnamaldehyde using Pd catalysts supported on Mg/Al mixed oxides: Influence of the Pd incorporation method. *Can. J. Chem. Eng.* **2018**, *96*, 297–306. [\[CrossRef\]](#)

51. Chen, H.-Y.; Chang, C.-T.; Chiang, S.-J.; Liaw, B.-J.; Chen, Y.-Z. Selective hydrogenation of crotonaldehyde in liquid-phase over Au/Mg₂AlO hydrotalcite catalysts. *Appl. Catal. A* **2010**, *381*, 209–215. [[CrossRef](#)]
52. Duan, J.; Wang, D.; Cui, R.; Zhang, H.; Zhang, B.; Guan, H.; Zhao, Y. In-situ incorporation of Pt nanoparticles on layered double hydroxides for selective conversion of cinnamaldehyde to cinnamyl alcohol. *ChemistrySelect* **2021**, *6*, 13890–13896. [[CrossRef](#)]
53. Tan, Y.; Liu, X.; Zhang, L.; Liu, F.; Wang, A.; Zhang, T. Producing of cinnamyl alcohol from cinnamaldehyde over supported gold nanocatalyst. *Chin. J. Catal.* **2021**, *42*, 470–481. [[CrossRef](#)]
54. Wang, H.; Lan, X.; Wang, S.; Ali, B.; Wang, T. Selective hydrogenation of 2-pentenal using highly dispersed pt catalysts supported on ZnSnAl mixed metal oxides derived from layered double hydroxides. *Catal. Sci. Technol.* **2020**, *10*, 1106–1116. [[CrossRef](#)]
55. Xiang, X.; He, W.; Xie, L.; Li, F. A mild solution chemistry method to synthesize hydrotalcite-supported platinum nanocrystals for selective hydrogenation of cinnamaldehyde in neat water. *Catal. Sci. Technol.* **2013**, *3*, 2819–2827. [[CrossRef](#)]
56. Hui, T.; Miao, C.; Feng, J.; Liu, Y.; Wang, Q.; Wang, Y.; Li, D. Atmosphere induced amorphous and permeable carbon layer encapsulating PtGa catalyst for selective cinnamaldehyde hydrogenation. *J. Catal.* **2020**, *389*, 229–240. [[CrossRef](#)]
57. Lin, W.; Cheng, H.; Li, X.; Zhang, C.; Zhao, F.; Arai, M. Layered double hydroxide-like Mg₃Al_{1-x}Fe_x materials as supports for ir catalysts: Promotional effects of Fe doping in selective hydrogenation of cinnamaldehyde. *Chin. J. Catal.* **2018**, *39*, 988–996. [[CrossRef](#)]
58. Miao, C.; Zhang, F.; Cai, L.; Hui, T.; Feng, J.; Li, D. Identification and insight into the role of ultrathin LDH-induced dual-interface sites for selective cinnamaldehyde hydrogenation. *ChemCatChem* **2021**, *13*, 4937–4947. [[CrossRef](#)]
59. Yang, Y.; Rao, D.; Chen, Y.; Dong, S.; Wang, B.; Zhang, X.; Wei, M. Selective hydrogenation of cinnamaldehyde over co-based intermetallic compounds derived from layered double hydroxides. *ACS Catal.* **2018**, *8*, 11749–11760. [[CrossRef](#)]
60. Yang, L.; Jiang, Z.; Fan, G.; Li, F. The promotional effect of ZnO addition to supported ni nanocatalysts from layered double hydroxide precursors on selective hydrogenation of citral. *Catal. Sci. Technol.* **2014**, *4*, 1123–1131. [[CrossRef](#)]
61. Zhou, J.; Yang, Y.; Li, C.; Zhang, S.; Chen, Y.; Shi, S.; Wei, M. Synthesis of Co–Sn intermetallic nanocatalysts toward selective hydrogenation of citral. *J. Mater. Chem. A* **2016**, *4*, 12825–12832. [[CrossRef](#)]
62. Li, W.; Fan, G.; Yang, L.; Li, F. Surface lewis acid-promoted copper-based nanocatalysts for highly efficient and chemoselective hydrogenation of citral to unsaturated allylic alcohols. *Catal. Sci. Technol.* **2016**, *6*, 2337–2348. [[CrossRef](#)]
63. Li, C.; Ke, C.; Han, R.; Fan, G.; Yang, L.; Li, F. The remarkable promotion of In Situ formed Pt-cobalt oxide interfacial sites on the carbonyl reduction to allylic alcohols. *Mol. Catal.* **2018**, *455*, 78–87. [[CrossRef](#)]
64. Wang, Y.; He, W.; Wang, L.; Yang, J.; Xiang, X.; Zhang, B.; Li, F. Highly active supported Pt nanocatalysts synthesized by alcohol reduction towards hydrogenation of cinnamaldehyde: Synergy of metal valence and hydroxyl groups. *Chem.—Asian J.* **2015**, *10*, 1561–1570. [[CrossRef](#)]
65. Rudolf, C.; Dragoi, B.; Ungureanu, A.; Chiriac, A.; Royer, S.; Nastro, A.; Dumitriu, E. Nial and coal materials derived from takovite-like LDHs and related structures as efficient chemoselective hydrogenation catalysts. *Catal. Sci. Technol.* **2014**, *4*, 179–189. [[CrossRef](#)]
66. Tauster, S.J.; Fung, S.C.; Garten, R.L. Strong metal-support interactions. Group 8 noble metals supported on titanium dioxide. *J. Am. Chem. Soc.* **1978**, *100*, 170–175. [[CrossRef](#)]
67. Liu, C.; Nan, C.; Fan, G.; Yang, L.; Li, F. Facile synthesis and synergistically acting catalytic performance of supported bimetallic pdni nanoparticle catalysts for selective hydrogenation of citral. *Mol. Catal.* **2017**, *436*, 237–247. [[CrossRef](#)]
68. Zhang, Y.; Wei, S.; Lin, Y.; Fan, G.; Li, F. Dispersing metallic platinum on green rust enables effective and selective hydrogenation of carbonyl group in cinnamaldehyde. *ACS Omega* **2018**, *3*, 12778–12787. [[CrossRef](#)]
69. Zhao, J.; Xu, S.; Wu, H.; You, Z.; Deng, L.; Qiu, X. Metal-support interactions on Ru/CaAlO_x catalysts derived from structural reconstruction of Ca–Al layered double hydroxides for ammonia decomposition. *Chem. Commun.* **2019**, *55*, 14410–14413. [[CrossRef](#)]
70. Miao, C.; Hui, T.; Liu, Y.; Feng, J.; Li, D. Pd/MgAl-LDH nanocatalyst with vacancy-rich sandwich structure: Insight into interfacial effect for selective hydrogenation. *J. Catal.* **2019**, *370*, 107–117. [[CrossRef](#)]
71. Han, R.; Nan, C.; Yang, L.; Fan, G.; Li, F. Direct synthesis of hybrid layered double hydroxide–carbon composites supported pd nanocatalysts efficient in selective hydrogenation of citral. *RSC Adv.* **2015**, *5*, 33199–33207. [[CrossRef](#)]
72. Chen, Y.; Liu, W.; Yin, P.; Ju, M.; Wang, J.; Yang, W.; Yang, Y.; Shen, C. Synergistic effect between Ni single atoms and acid–base sites: Mechanism investigation into catalytic transfer hydrogenation reaction. *J. Catal.* **2021**, *393*, 1–10. [[CrossRef](#)]
73. Basu, S.; Pradhan, N.C. Kinetics of acetone hydrogenation for synthesis of isopropyl alcohol over cu-al mixed oxide catalysts. *Catal. Today* **2020**, *348*, 118–126. [[CrossRef](#)]
74. Santiago-Pedro, S.; Tamayo-Galván, V.; Viveros-García, T. Effect of the acid–base properties of the support on the performance of Pt catalysts in the partial hydrogenation of citral. *Catal. Today* **2013**, *213*, 101–108. [[CrossRef](#)]
75. Shen, M.; Zhao, G.; Nie, Q.; Meng, C.; Sun, W.; Si, J.; Liu, Y.; Lu, Y. Ni-foam-structured Ni–Al₂O₃ ensemble as an efficient catalyst for gas-phase acetone hydrogenation to isopropanol. *ACS Appl. Mater. Interfaces* **2021**, *13*, 28334–28347. [[CrossRef](#)] [[PubMed](#)]
76. Jaswal, A.; Singh, P.P.; Mondal, T. Furfural—A versatile, biomass-derived platform chemical for the production of renewable chemicals. *Green Chem.* **2022**, *24*, 510–551. [[CrossRef](#)]
77. Chen, S.; Wojcieszak, R.; Dumeignil, F.; Marceau, E.; Royer, S. How catalysts and experimental conditions determine the selective hydroconversion of furfural and 5-hydroxymethylfurfural. *Chem. Rev.* **2018**, *118*, 11023–11117. [[CrossRef](#)] [[PubMed](#)]

78. Mariscal, R.; Maireles-Torres, P.; Ojeda, M.; Sadaba, I.; Lopez Granados, M. Furfural: A renewable and versatile platform molecule for the synthesis of chemicals and fuels. *Energy Environ. Sci.* **2016**, *9*, 1144–1189. [[CrossRef](#)]
79. Li, X.; Liu, T.; Shao, S.; Yan, J.; Zhang, H.; Cai, Y. Catalytic transfer hydrogenation of biomass-derived oxygenated chemicals over hydrotalcite-like copper catalyst using methanol as hydrogen donor. *Biomass Convers. Biorefin.* **2022**. [[CrossRef](#)]
80. Zhang, J.; Chen, J. Selective transfer hydrogenation of biomass-based furfural and 5-hydroxymethylfurfural over hydrotalcite-derived copper catalysts using methanol as a hydrogen donor. *ACS Sustain. Chem. Eng.* **2017**, *5*, 5982–5993. [[CrossRef](#)]
81. Yan, K.; Chen, A. Efficient hydrogenation of biomass-derived furfural and levulinic acid on the facilely synthesized noble-metal-free Cu–Cr catalyst. *Energy* **2013**, *58*, 357–363. [[CrossRef](#)]
82. Yan, K.; Liao, J.; Wu, X.; Xie, X. A noble-metal free Cu-catalyst derived from hydrotalcite for highly efficient hydrogenation of biomass-derived furfural and levulinic acid. *RSC Adv.* **2013**, *3*, 3853–3856. [[CrossRef](#)]
83. Ramos, R.; Peixoto, A.F.; Arias-Serrano, B.I.; Soares, O.S.G.P.; Pereira, M.F.R.; Kubička, D.; Freire, C. Catalytic transfer hydrogenation of furfural over $\text{Co}_3\text{O}_4\text{--Al}_2\text{O}_3$ hydrotalcite-derived catalyst. *ChemCatChem* **2020**, *12*, 1467–1475. [[CrossRef](#)]
84. Pan, Z.; Jiang, H.; Gong, B.; Luo, R.; Zhang, W.; Wang, G.-H. Layered double hydroxide derived nickel-oxide hollow nanospheres for selective transfer hydrogenation with improved stability. *J. Mater. Chem. A* **2020**, *8*, 23376–23384. [[CrossRef](#)]
85. Yang, Y.; Chen, L.; Chen, Y.; Liu, W.; Feng, H.; Wang, B.; Zhang, X.; Wei, M. The selective hydrogenation of furfural over intermetallic compounds with outstanding catalytic performance. *Green Chem.* **2019**, *21*, 5352–5362. [[CrossRef](#)]
86. Luo, L.; Yuan, F.; Zaera, F.; Zhu, Y. Catalytic hydrogenation of furfural to furfuryl alcohol on hydrotalcite-derived $\text{Cu}_x\text{Ni}_{3-x}\text{AlO}_y$ mixed-metal oxides. *J. Catal.* **2021**, *404*, 420–429. [[CrossRef](#)]
87. Aldureid, A.; Medina, F.; Patience, G.S.; Montané, D. Ni-Cu/ Al_2O_3 from layered double hydroxides hydrogenates furfural to alcohols. *Catalysts* **2022**, *12*, 390. [[CrossRef](#)]
88. Manikandan, M.; Venugopal, A.K.; Prabu, K.; Jha, R.K.; Thirumalaiswamy, R. Role of surface synergistic effect on the performance of Ni-based hydrotalcite catalyst for highly efficient hydrogenation of furfural. *J. Mol. Catal. A Chem.* **2016**, *417*, 153–162. [[CrossRef](#)]
89. Villaverde, M.M.; Bertero, N.M.; Garetto, T.F.; Marchi, A.J. Selective liquid-phase hydrogenation of furfural to furfuryl alcohol over Cu-based catalysts. *Catal. Today* **2013**, *213*, 87–92. [[CrossRef](#)]
90. Villaverde, M.M.; Garetto, T.F.; Marchi, A.J. Liquid-phase transfer hydrogenation of furfural to furfuryl alcohol on Cu-Mg-Al catalysts. *Catal. Commun.* **2015**, *58*, 6–10. [[CrossRef](#)]
91. Xu, C.; Zheng, L.; Liu, J.; Huang, Z. Furfural hydrogenation on nickel-promoted Cu-containing catalysts prepared from hydrotalcite-like precursors. *Chin. J. Chem.* **2011**, *29*, 691–697. [[CrossRef](#)]
92. Xu, C.; Zheng, L.; Deng, D.; Liu, J.; Liu, S. Effect of activation temperature on the surface copper particles and catalytic properties of Cu–Ni–Mg–Al oxides from hydrotalcite-like precursors. *Catal. Commun.* **2011**, *12*, 996–999. [[CrossRef](#)]
93. Wu, J.; Gao, G.; Li, J.; Sun, P.; Long, X.; Li, F. Efficient and versatile CuNi alloy nanocatalysts for the highly selective hydrogenation of furfural. *Appl. Catal. B* **2017**, *203*, 227–236. [[CrossRef](#)]
94. Kang, S.; Fu, J.; Zhang, G. From lignocellulosic biomass to levulinic acid: A review on acid-catalyzed hydrolysis. *Renew. Sustain. Energy Rev.* **2018**, *94*, 340–362. [[CrossRef](#)]
95. Yan, K.; Yang, Y.; Chai, J.; Lu, Y. Catalytic reactions of gamma-valerolactone: A platform to fuels and value-added chemicals. *Appl. Catal. B* **2015**, *179*, 292–304. [[CrossRef](#)]
96. Shao, Y.; Sun, K.; Li, Q.; Liu, Q.; Zhang, S.; Liu, Q.; Hu, G.; Hu, X. Copper-based catalysts with tunable acidic and basic sites for the selective conversion of levulinic acid/ester to γ -valerolactone or 1,4-pentanediol. *Green Chem.* **2019**, *21*, 4499–4511. [[CrossRef](#)]
97. Li, W.; Fan, G.; Yang, L.; Li, F. Highly efficient vapor-phase hydrogenation of biomass-derived levulinic acid over structured nanowall-like nickel-based catalyst. *ChemCatChem* **2016**, *8*, 2724–2733. [[CrossRef](#)]
98. Gundeboina, R.; Gadasandula, S.; Velisoju, V.K.; Gutta, N.; Kotha, L.R.; Aytam, H.P. Ni-Al-Ti hydrotalcite based catalyst for the selective hydrogenation of biomass-derived levulinic acid to γ -valerolactone. *ChemistrySelect* **2019**, *4*, 202–210. [[CrossRef](#)]
99. Yan, K.; Chen, A. Selective hydrogenation of furfural and levulinic acid to biofuels on the ecofriendly Cu–Fe catalyst. *Fuel* **2014**, *115*, 101–108. [[CrossRef](#)]
100. Zhang, J.; Chen, J.; Guo, Y.; Chen, L. Effective upgrade of levulinic acid into γ -valerolactone over an inexpensive and magnetic catalyst derived from hydrotalcite precursor. *ACS Sustain. Chem. Eng.* **2015**, *3*, 1708–1714. [[CrossRef](#)]
101. Shao, Y.; Sun, K.; Fan, M.; Wang, J.; Gao, G.; Zhang, L.; Zhang, S.; Hu, X. Selective conversion of levulinic acid to gamma-valerolactone over Ni-based catalysts: Impacts of catalyst formulation on sintering of nickel. *Chem. Eng. Sci.* **2022**, *248*, 117258. [[CrossRef](#)]
102. Gundeboina, R.; Velisoju, V.K.; Gutta, N.; Medak, S.; Aytam, H.P. Influence of surface Lewis acid sites for the selective hydrogenation of levulinic acid to γ -valerolactone over Ni–Cu–Al mixed oxide catalyst. *React. Kinet. Mech. Catal.* **2019**, *127*, 601–616. [[CrossRef](#)]
103. Long, X.; Sun, P.; Li, Z.; Lang, R.; Xia, C.; Li, F. Magnetic Co/ Al_2O_3 catalyst derived from hydrotalcite for hydrogenation of levulinic acid to γ -valerolactone. *Chin. J. Catal.* **2015**, *36*, 1512–1518. [[CrossRef](#)]
104. Wang, L.; Yang, Y.; Yin, P.; Ren, Z.; Liu, W.; Tian, Z.; Zhang, Y.; Xu, E.; Yin, J.; Wei, M. Moox-decorated Co-based catalysts toward the hydrodeoxygenation reaction of biomass-derived platform molecules. *ACS Appl. Mater. Interfaces* **2021**, *13*, 31799–31807. [[CrossRef](#)] [[PubMed](#)]

105. Gupta, S.S.R.; Kantam, M.L. Selective hydrogenation of levulinic acid into γ -valerolactone over Cu/Ni hydrotalcite-derived catalyst. *Catal. Today* **2018**, *309*, 189–194. [[CrossRef](#)]
106. Siddiqui, N.; Pendem, C.; Goyal, R.; Khatun, R.; Khan, T.S.; Samanta, C.; Chiang, K.; Shah, K.; Ali Haider, M.; Bal, R. Study of γ -valerolactone production from hydrogenation of levulinic acid over nanostructured pt-hydrotalcite catalysts at low temperature. *Fuel* **2022**, *323*, 124272. [[CrossRef](#)]
107. Swarna Jaya, V.; Sudhakar, M.; Naveen Kumar, S.; Venugopal, A. Selective hydrogenation of levulinic acid to γ -valerolactone over a Ru/Mg–LaO catalyst. *RSC Adv.* **2015**, *5*, 9044–9049. [[CrossRef](#)]
108. Abdelrahman, O.A.; Luo, H.Y.; Heyden, A.; Román-Leshkov, Y.; Bond, J.Q. Toward rational design of stable, supported metal catalysts for aqueous-phase processing: Insights from the hydrogenation of levulinic acid. *J. Catal.* **2015**, *329*, 10–21. [[CrossRef](#)]
109. Wright, W.R.H.; Palkovits, R. Development of heterogeneous catalysts for the conversion of levulinic acid to γ -valerolactone. *ChemSusChem* **2012**, *5*, 1657–1667. [[CrossRef](#)]
110. Varkolu, M.; Velpula, V.; Burri, D.R.; Kamaraju, S.R.R. Gas phase hydrogenation of levulinic acid to γ -valerolactone over supported Ni catalysts with formic acid as hydrogen source. *N. J. Chem.* **2016**, *40*, 3261–3267. [[CrossRef](#)]
111. Li, D.; Tian, Z.; Cai, X.; Li, Z.; Zhang, C.; Zhang, W.; Song, Y.; Wang, H.; Li, C. Nature of polymeric condensates during furfural rearrangement to cyclopentanone and cyclopentanol over Cu-based catalysts. *N. J. Chem.* **2021**, *45*, 22767–22777. [[CrossRef](#)]
112. Gundekari, S.; Srinivasan, K. In Situ generated Ni(0)@boehmite from NiAl-LDH: An efficient catalyst for selective hydrogenation of biomass derived levulinic acid to γ -valerolactone. *Catal. Commun.* **2017**, *102*, 40–43. [[CrossRef](#)]
113. Hussain, S.; Velisoju, V.K.; Rajan, N.P.; Kumar, B.P.; Chary, K.V.R. Synthesis of γ -valerolactone from levulinic acid and formic acid over Mg–Al hydrotalcite like compound. *ChemistrySelect* **2018**, *3*, 6186–6194. [[CrossRef](#)]
114. Mitta, H.; Seelam, P.K.; Chary, K.V.R.; Mutyala, S.; Boddula, R.; Inamuddin; Asiri, A.M. Efficient vapor-phase selective hydrogenolysis of bio-levulinic acid to γ -valerolactone using Cu supported on hydrotalcite catalysts. *Glob. Chall.* **2018**, *2*, 1800028. [[CrossRef](#)]
115. Alonso, D.M.; Wettstein, S.G.; Dumesic, J.A. Bimetallic catalysts for upgrading of biomass to fuels and chemicals. *Chem. Soc. Rev.* **2012**, *41*, 8075–8098. [[CrossRef](#)]
116. Werpy, T.; Petersen, G.; Aden, A.; Bozell, J.; Holladay, J.; White, J.; Manheim, A.; Eliot, D.; Lasure, L.; Jones, S. *Top Value Added Chemicals from Biomass: Volume 1—Results of Screening for Potential Candidates from Sugars and Synthesis Gas*; DTIC Document; DTIC: Fort Belvoir, VA, USA, 2004.
117. Yamaguchi, S.; Fujita, S.; Nakajima, K.; Yamazoe, S.; Yamasaki, J.; Mizugaki, T.; Mitsudome, T. Air-stable and reusable nickel phosphide nanoparticle catalyst for the highly selective hydrogenation of d-glucose to d-sorbitol. *Green Chem.* **2021**, *23*, 2010–2016. [[CrossRef](#)]
118. Yamaguchi, S.; Mizugaki, T.; Mitsudome, T. Efficient d-xylose hydrogenation to d-xylitol over a hydrotalcite-supported nickel phosphide nanoparticle catalyst. *Eur. J. Inorg. Chem.* **2021**, *2021*, 3327–3331. [[CrossRef](#)]
119. Yamaguchi, S.; Fujita, S.; Nakajima, K.; Yamazoe, S.; Yamasaki, J.; Mizugaki, T.; Mitsudome, T. Support-boosted nickel phosphide nanoalloy catalysis in the selective hydrogenation of maltose to maltitol. *ACS Sustain. Chem. Eng.* **2021**, *9*, 6347–6354. [[CrossRef](#)]
120. Tathod, A.; Kane, T.; Sanil, E.S.; Dhepe, P.L. Solid base supported metal catalysts for the oxidation and hydrogenation of sugars. *J. Mol. Catal. A Chem.* **2014**, *388*, 90–99. [[CrossRef](#)]
121. Attia, S.; Schmidt, M.C.; Schröder, C.; Weber, J.; Baumann, A.-K.; Schauerermann, S. Keto–enol tautomerization as a first step in hydrogenation of carbonyl compounds. *J. Phys. Chem. C* **2019**, *123*, 29271–29277. [[CrossRef](#)]
122. Zhang, J.; Wu, S.; Liu, Y.; Li, B. Hydrogenation of glucose over reduced Ni/Cu/Al hydrotalcite precursors. *Catal. Commun.* **2013**, *35*, 23–26. [[CrossRef](#)]
123. Zhang, J.; Xu, S.; Wu, S.; Liu, Y. Hydrogenation of fructose over magnetic catalyst derived from hydrotalcite precursor. *Chem. Eng. Sci.* **2013**, *99*, 171–176. [[CrossRef](#)]
124. Scholz, D.; Aellig, C.; Mondelli, C.; Pérez-Ramírez, J. Continuous transfer hydrogenation of sugars to alditols with bioderived donors over Cu–Ni–Al catalysts. *ChemCatChem* **2015**, *7*, 1551–1558. [[CrossRef](#)]
125. McCue, A.J.; Anderson, J.A. Recent advances in selective acetylene hydrogenation using palladium containing catalysts. *Front. Chem. Sci. Eng.* **2015**, *9*, 142–153. [[CrossRef](#)]
126. Kim, W.-J.; Moon, S.H. Modified Pd catalysts for the selective hydrogenation of acetylene. *Catal. Today* **2012**, *185*, 2–16. [[CrossRef](#)]
127. Feng, J.-T.; Ma, X.-Y.; Evans, D.G.; Li, D.-Q. Enhancement of metal dispersion and selective acetylene hydrogenation catalytic properties of a supported Pd catalyst. *Ind. Eng. Chem. Res.* **2011**, *50*, 1947–1954. [[CrossRef](#)]
128. Ma, X.-Y.; Chai, Y.-Y.; Evans, D.G.; Li, D.-Q.; Feng, J.-T. Preparation and selective acetylene hydrogenation catalytic properties of supported Pd catalyst by the In Situ precipitation–reduction method. *J. Phys. Chem. C* **2011**, *115*, 8693–8701. [[CrossRef](#)]
129. He, Y.; Fan, J.; Feng, J.; Luo, C.; Yang, P.; Li, D. Pd nanoparticles on hydrotalcite as an efficient catalyst for partial hydrogenation of acetylene: Effect of support acidic and basic properties. *J. Catal.* **2015**, *331*, 118–127. [[CrossRef](#)]
130. Liu, Y.; He, Y.; Zhou, D.; Feng, J.; Li, D. Catalytic performance of Pd-promoted Cu hydrotalcite-derived catalysts in partial hydrogenation of acetylene: Effect of Pd–Cu alloy formation. *Catal. Sci. Technol.* **2016**, *6*, 3027–3037. [[CrossRef](#)]
131. Gao, X.; Zhou, Y.; Jing, F.; Luo, J.; Huang, Q.; Chu, W. Layered double hydroxides derived ZnO–Al₂O₃ supported Pd–Ag catalysts for selective hydrogenation of acetylene. *Chin. J. Chem.* **2017**, *35*, 1009–1015. [[CrossRef](#)]
132. Liu, Y.N.; Feng, J.T.; He, Y.F.; Sun, J.H.; Li, D.Q. Partial hydrogenation of acetylene over a NiTi-layered double hydroxide supported PdAg catalyst. *Catal. Sci. Technol.* **2015**, *5*, 1231–1240. [[CrossRef](#)]

133. Liu, Y.; Zhao, J.; He, Y.; Feng, J.; Wu, T.; Li, D. Highly efficient pdag catalyst using a reducible Mg-Ti mixed oxide for selective hydrogenation of acetylene: Role of acidic and basic sites. *J. Catal.* **2017**, *348*, 135–145. [CrossRef]
134. Rives, V.; Labajos, F.M.; Trujillano, R.; Romeo, E.; Royo, C.; Monzón, A. Acetylene hydrogenation on Ni–Al–Cr oxide catalysts: The role of added Zn. *Appl. Clay Sci.* **1998**, *13*, 363–379. [CrossRef]
135. Monzón, A.; Romeo, E.; Royo, C.; Trujillano, R.; Labajos, F.M.; Rives, V. Use of hydrotalcites as catalytic precursors of multimetallic mixed oxides. Application in the hydrogenation of acetylene. *Appl. Catal. A* **1999**, *185*, 53–63. [CrossRef]
136. Liu, Y.; Zhao, J.; Feng, J.; He, Y.; Du, Y.; Li, D. Layered double hydroxide-derived Ni-Cu nanoalloy catalysts for semi-hydrogenation of alkynes: Improvement of selectivity and anti-coking ability via alloying of Ni and Cu. *J. Catal.* **2018**, *359*, 251–260. [CrossRef]
137. Bridier, B.; Pérez-Ramírez, J. Cooperative effects in ternary Cu-Ni-Fe catalysts lead to enhanced alkene selectivity in alkyne hydrogenation. *J. Am. Chem. Soc.* **2010**, *132*, 4321–4327. [CrossRef] [PubMed]
138. Fu, F.; Liu, Y.; Li, Y.; Fu, B.; Zheng, L.; Feng, J.; Li, D. Interfacial bifunctional effect promoted non-noble Cu/FeYMgO_x catalysts for selective hydrogenation of acetylene. *ACS Catal.* **2021**, *11*, 11117–11128. [CrossRef]
139. Mastalir, Á.; Király, Z. Pd nanoparticles in hydrotalcite: Mild and highly selective catalysts for alkyne semihydrogenation. *J. Catal.* **2003**, *220*, 372–381. [CrossRef]
140. Chen, Y.; Li, C.; Zhou, J.; Zhang, S.; Rao, D.; He, S.; Wei, M.; Evans, D.G.; Duan, X. Metal phosphides derived from hydrotalcite precursors toward the selective hydrogenation of phenylacetylene. *ACS Catal.* **2015**, *5*, 5756–5765. [CrossRef]
141. Cooper, B.H.; Donnis, B.B.L. Aromatic saturation of distillates: An overview. *Appl. Catal. A* **1996**, *137*, 203–223. [CrossRef]
142. Stanislaus, A.; Cooper, B.H. Aromatic hydrogenation catalysis: A review. *Catal. Rev.* **1994**, *36*, 75–123. [CrossRef]
143. Kim, K.-H.; Jahan, S.A.; Kabir, E.; Brown, R.J.C. A review of airborne polycyclic aromatic hydrocarbons (pahs) and their human health effects. *Environ. Int.* **2013**, *60*, 71–80. [CrossRef]
144. Qi, S.-C.; Wei, X.-Y.; Zong, Z.-M.; Wang, Y.-K. Application of supported metallic catalysts in catalytic hydrogenation of arenes. *RSC Adv.* **2013**, *3*, 14219–14232. [CrossRef]
145. Sun, Z.H.; Fridrich, B.; de Santi, A.; Elangovan, S.; Barta, K. Bright side of lignin depolymerization: Toward new platform chemicals. *Chem. Rev.* **2018**, *118*, 614–678. [CrossRef]
146. Zhu, T.; Dong, J.; Niu, L.; Chen, G.; Ricardez-Sandoval, L.; Wen, X.; Bai, G. Highly dispersed ni/nicaalox nanocatalyst derived from ternary layered double hydroxides for phenol hydrogenation: Spatial confinement effects and basicity of the support. *Appl. Clay Sci.* **2021**, *203*, 106003. [CrossRef]
147. Dong, J.; Wen, X.; Zhu, T.; Qin, J.; Wu, Z.; Chen, L.; Bai, G. Hierarchically nanostructured bimetallic NiCo/Mg_xNiYO catalyst with enhanced activity for phenol hydrogenation. *Mol. Catal.* **2020**, *485*, 110846. [CrossRef]
148. Dong, J.; Zhu, T.; Li, H.; Sun, H.; Wang, Y.; Niu, L.; Wen, X.; Bai, G. Biotemplate-assisted synthesis of layered double oxides confining ultrafine Ni nanoparticles as a stable catalyst for phenol hydrogenation. *Ind. Eng. Chem. Res.* **2019**, *58*, 14688–14694. [CrossRef]
149. Li, H.; Wang, X.; Liu, Y.; He, Y.; Feng, J.; Li, D. Pd nanoparticles loaded on coalce layered double oxide nanosheets for phenol hydrogenation. *ACS Appl. Nano Mater.* **2021**, *4*, 11820–11829. [CrossRef]
150. Sreenavya, A.; Sahu, A.; Sakthivel, A. Hydrogenation of lignin-derived phenolic compound eugenol over ruthenium-containing nickel hydrotalcite-type materials. *Ind. Eng. Chem. Res.* **2020**, *59*, 11979–11990. [CrossRef]
151. Liu, M.; Zhang, J.; Zheng, L.; Fan, G.; Yang, L.; Li, F. Significant promotion of surface oxygen vacancies on bimetallic coninanocatalysts for hydrodeoxygenation of biomass-derived vanillin to produce methylcyclohexanol. *ACS Sustain. Chem. Eng.* **2020**, *8*, 6075–6089. [CrossRef]
152. Ramirez-Verduzco, L.F.; Rodriguez-Rodríguez, J.E.; Jaramillo-Jacob, A.d.R. Predicting cetane number, kinematic viscosity, density and higher heating value of biodiesel from its fatty acid methyl ester composition. *Fuel* **2012**, *91*, 102–111. [CrossRef]
153. Cao, X.; Long, F.; Wang, F.; Zhao, J.; Xu, J.; Jiang, J. Chemoselective decarboxylation of higher aliphatic esters to diesel-range alkanes over the NiCu/Al₂O₃ bifunctional catalyst under mild reaction conditions. *Renew. Energy* **2021**, *180*, 1–13. [CrossRef]
154. Zhao, N.; Zheng, Y.; Chen, J. Remarkably reducing carbon loss and H₂ consumption on Ni–Ga intermetallic compounds in deoxygenation of methyl esters to hydrocarbons. *J. Energy Chem.* **2020**, *41*, 194–208. [CrossRef]
155. Cui, G.; Zhang, X.; Wang, H.; Li, Z.; Wang, W.; Yu, Q.; Zheng, L.; Wang, Y.; Zhu, J.; Wei, M. ZrO_{2-x} modified Cu nanocatalysts with synergistic catalysis towards carbon-oxygen bond hydrogenation. *Appl. Catal. B* **2021**, *280*, 119406. [CrossRef]
156. Li, C.Z.; Zhao, X.C.; Wang, A.Q.; Huber, G.W.; Zhang, T. Catalytic transformation of lignin for the production of chemicals and fuels. *Chem. Rev.* **2015**, *115*, 11559–11624. [CrossRef] [PubMed]
157. Bajwa, D.S.; Pourhashem, G.; Ullah, A.H.; Bajwa, S.G. A concise review of current lignin production, applications, products and their environmental impact. *Ind. Crops Prod.* **2019**, *139*, 111526. [CrossRef]
158. Jia, Z.; Ji, N.; Diao, X.; Li, X.; Zhao, Y.; Lu, X.; Liu, Q.; Liu, C.; Chen, G.; Ma, L.; et al. Highly selective hydrodeoxygenation of lignin to naphthenes over three-dimensional flower-like Ni₂P derived from hydrotalcite. *ACS Catal.* **2022**, *12*, 1338–1356. [CrossRef]
159. Yue, X.; Zhang, L.; Sun, L.; Gao, S.; Gao, W.; Cheng, X.; Shang, N.; Gao, Y.; Wang, C. Highly efficient hydrodeoxygenation of lignin-derivatives over ni-based catalyst. *Appl. Catal. B* **2021**, *293*, 120243. [CrossRef]
160. Wang, Z.; Wang, A.; Yang, L.; Fan, G.; Li, F. Supported Ru nanocatalyst over phosphotungstate intercalated Zn-Al layered double hydroxide derived mixed metal oxides for efficient hydrodeoxygenation of guaiacol. *Mol. Catal.* **2022**, *528*, 112503. [CrossRef]
161. Xu, Q.; Shi, Y.; Yang, L.; Fan, G.; Li, F. The promotional effect of surface Ru decoration on the catalytic performance of Co-based nanocatalysts for guaiacol hydrodeoxygenation. *Mol. Catal.* **2020**, *497*, 111224. [CrossRef]

162. De Saegher, T.; Lauwaert, J.; Hanssen, J.; Bruneel, E.; Van Zele, M.; Van Geem, K.; De Buysser, K.; Verberckmoes, A. Monometallic cerium layered double hydroxide supported Pd-Ni nanoparticles as high performance catalysts for lignin hydrogenolysis. *Materials* **2020**, *13*, 691. [CrossRef]
163. Du, B.; Chen, C.; Sun, Y.; Liu, B.; Yang, Y.; Gao, S.; Zhang, Z.; Wang, X.; Zhou, J. Ni-Mg-Al catalysts effectively promote depolymerization of rice husk lignin to bio-oil. *Catal. Lett.* **2020**, *150*, 1591–1604. [CrossRef]
164. Wang, M.; Zhang, X.; Li, H.; Lu, J.; Liu, M.; Wang, F. Carbon modification of nickel catalyst for depolymerization of oxidized lignin to aromatics. *ACS Catal.* **2018**, *8*, 1614–1620. [CrossRef]
165. Wang, H.-T.; Li, Z.-K.; Yan, H.-L.; Lei, Z.-P.; Yan, J.-C.; Ren, S.-B.; Wang, Z.-C.; Kang, S.-G.; Shui, H.-F. Catalytic hydrogenolysis of lignin and model compounds over highly dispersed Ni-Ru/Al₂O₃ without additional H₂. *Fuel* **2022**, *326*, 125027. [CrossRef]
166. Kruger, J.S.; Cleveland, N.S.; Zhang, S.; Katahira, R.; Black, B.A.; Chupka, G.M.; Lammens, T.; Hamilton, P.G.; Bidy, M.J.; Beckham, G.T. Lignin depolymerization with nitrate-intercalated hydrotalcite catalysts. *ACS Catal.* **2016**, *6*, 1316–1328. [CrossRef]
167. Adkins, H.; Connor, R. The catalytic hydrogenation of organic compounds over copper chromite. *J. Am. Chem. Soc.* **1931**, *53*, 1091–1095. [CrossRef]
168. Xu, W.; Wang, H.; Liu, X.; Ren, J.; Wang, Y.; Lu, G. Direct catalytic conversion of furfural to 1,5-pentanediol by hydrogenolysis of the furan ring under mild conditions over Pt/CO₂AlO₄ catalyst. *Chem. Commun.* **2011**, *47*, 3924–3926. [CrossRef]
169. Mizugaki, T.; Yamakawa, T.; Nagatsu, Y.; Maeno, Z.; Mitsudome, T.; Jitsukawa, K.; Kaneda, K. Direct transformation of furfural to 1,2-pentanediol using a hydrotalcite-supported platinum nanoparticle catalyst. *ACS Sustain. Chem. Eng.* **2014**, *2*, 2243–2247. [CrossRef]
170. Liu, H.; Huang, Z.; Zhao, F.; Cui, F.; Li, X.; Xia, C.; Chen, J. Efficient hydrogenolysis of biomass-derived furfuryl alcohol to 1,2- and 1,5-pentanediols over a non-precious Cu-Mg₃AlO_{4.5} bifunctional catalyst. *Catal. Sci. Technol.* **2016**, *6*, 668–671. [CrossRef]
171. Liu, H.; Huang, Z.; Kang, H.; Xia, C.; Chen, J. Selective hydrogenolysis of biomass-derived furfuryl alcohol into 1,2- and 1,5-pentanediol over highly dispersed Cu-Al₂O₃ catalysts. *Chin. J. Catal.* **2016**, *37*, 700–710. [CrossRef]
172. Sulmonetti, T.P.; Hu, B.; Lee, S.; Agrawal, P.K.; Jones, C.W. Reduced Cu-Co-Al mixed metal oxides for the ring-opening of furfuryl alcohol to produce renewable diols. *ACS Sustain. Chem. Eng.* **2017**, *5*, 8959–8969. [CrossRef]
173. Tan, J.; Su, Y.; Hai, X.; Huang, L.; Cui, J.; Zhu, Y.; Wang, Y.; Zhao, Y. Conversion of furfuryl alcohol to 1,5-pentanediol over Cu-coal nanocatalyst: The synergistic catalysis between Cu, CoO_x and the basicity of metal oxides. *Mol. Catal.* **2022**, *526*, 112391. [CrossRef]
174. Shao, Y.; Wang, J.; Du, H.; Sun, K.; Zhang, Z.; Zhang, L.; Li, Q.; Zhang, S.; Liu, Q.; Hu, X. Importance of magnesium in Cu-based catalysts for selective conversion of biomass-derived furan compounds to diols. *ACS Sustain. Chem. Eng.* **2020**, *8*, 5217–5228. [CrossRef]
175. Zhu, Y.; Zhao, W.; Zhang, J.; An, Z.; Ma, X.; Zhang, Z.; Jiang, Y.; Zheng, L.; Shu, X.; Song, H.; et al. Selective activation of C–OH, C–O–C, or C=C in furfuryl alcohol by engineered Pt sites supported on layered double oxides. *ACS Catal.* **2020**, *10*, 8032–8041. [CrossRef]
176. Shao, Y.; Wang, J.; Sun, K.; Gao, G.; Li, C.; Zhang, L.; Zhang, S.; Xu, L.; Hu, G.; Hu, X. Selective hydrogenation of furfural and its derivative over bimetallic Ni-Fe-based catalysts: Understanding the synergy between Ni sites and Ni-Fe alloy. *Renew. Energy* **2021**, *170*, 1114–1128. [CrossRef]
177. Shao, Y.; Guo, M.; Wang, J.; Sun, K.; Zhang, L.; Zhang, S.; Hu, G.; Xu, L.; Yuan, X.; Hu, X. Selective conversion of furfural into diols over Co-based catalysts: Importance of the coordination of hydrogenation sites and basic sites. *Ind. Eng. Chem. Res.* **2021**, *60*, 10393–10406. [CrossRef]
178. Roman-Leshkov, Y.; Barrett, C.J.; Liu, Z.Y.; Dumesic, J.A. Production of dimethylfuran for liquid fuels from biomass-derived carbohydrates. *Nature* **2007**, *447*, 982–985. [CrossRef]
179. Hoang, A.T.; Ölçer, A.I.; Nižetić, S. Prospective review on the application of biofuel 2,5-dimethylfuran to diesel engine. *J. Energy Inst.* **2021**, *94*, 360–386. [CrossRef]
180. Perret, N.; Grigoropoulos, A.; Zanella, M.; Manning, T.D.; Claridge, J.B.; Rosseinsky, M.J. Catalytic response and stability of nickel/alumina for the hydrogenation of 5-hydroxymethylfurfural in water. *ChemSusChem* **2016**, *9*, 521–531. [CrossRef]
181. Nagpure, A.S.; Venugopal, A.K.; Lucas, N.; Manikandan, M.; Thirumalaiswamy, R.; Chilukuri, S. Renewable fuels from biomass-derived compounds: Ru-containing hydrotalcites as catalysts for conversion of hmf to 2,5-dimethylfuran. *Catal. Sci. Technol.* **2015**, *5*, 1463–1472. [CrossRef]
182. Kong, X.; Zheng, R.; Zhu, Y.; Ding, G.; Zhu, Y.; Li, Y.-W. Rational design of Ni-based catalysts derived from hydrotalcite for selective hydrogenation of 5-hydroxymethylfurfural. *Green Chem.* **2015**, *17*, 2504–2514. [CrossRef]
183. Hansen, T.S.; Barta, K.; Anastas, P.T.; Ford, P.C.; Riisager, A. One-pot reduction of 5-hydroxymethylfurfural via hydrogen transfer from supercritical methanol. *Green Chem.* **2012**, *14*, 2457–2461. [CrossRef]
184. Kumalaputri, A.J.; Bottari, G.; Erne, P.M.; Heeres, H.J.; Barta, K. Tunable and selective conversion of 5-hmf to 2,5-furandimethanol and 2,5-dimethylfuran over copper-doped porous metal oxides. *ChemSusChem* **2014**, *7*, 2266–2275. [CrossRef] [PubMed]
185. Gupta, D.; Kumar, R.; Pant, K.K. Hydrotalcite supported bimetallic (Ni-Cu) catalyst: A smart choice for one-pot conversion of biomass-derived platform chemicals to hydrogenated biofuels. *Fuel* **2020**, *277*, 118111. [CrossRef]
186. An, Z.; Wang, W.; Dong, S.; He, J. Well-distributed cobalt-based catalysts derived from layered double hydroxides for efficient selective hydrogenation of 5-hydroxymethylfurfural to 2,5-methylfuran. *Catal. Today* **2019**, *319*, 128–138. [CrossRef]

187. Xia, J.; Gao, D.; Han, F.; Lv, R.; Waterhouse, G.I.N.; Li, Y. Hydrogenolysis of 5-hydroxymethylfurfural to 2,5-dimethylfuran over a modified coal-hydroxalcalite catalyst. *Front. Chem.* **2022**, *10*, 907649. [[CrossRef](#)]
188. Wang, Q.; Yu, Z.; Feng, J.; Fornasiero, P.; He, Y.; Li, D. Insight into the effect of dual active Cu⁰/Cu⁺ sites in a Cu/ZnO-Al₂O₃ catalyst on 5-hydroxymethylfurfural hydrodeoxygenation. *ACS Sustain. Chem. Eng.* **2020**, *8*, 15288–15298. [[CrossRef](#)]
189. Ma, N.; Song, Y.; Han, F.; Waterhouse, G.I.N.; Li, Y.; Ai, S. Highly selective hydrogenation of 5-hydroxymethylfurfural to 2,5-dimethylfuran at low temperature over a Co–N–C/NiAl–MMO catalyst. *Catal. Sci. Technol.* **2020**, *10*, 4010–4018. [[CrossRef](#)]
190. Kong, X.; Zhu, Y.; Zheng, H.; Zhu, Y.; Fang, Z. Inclusion of Zn into metallic Ni enables selective and effective synthesis of 2,5-dimethylfuran from bioderived 5-hydroxymethylfurfural. *ACS Sustain. Chem. Eng.* **2017**, *5*, 11280–11289. [[CrossRef](#)]
191. Wang, Q.; Feng, J.; Zheng, L.; Wang, B.; Bi, R.; He, Y.; Liu, H.; Li, D. Interfacial structure-determined reaction pathway and selectivity for 5-(hydroxymethyl)furfural hydrogenation over Cu-based catalysts. *ACS Catal.* **2020**, *10*, 1353–1365. [[CrossRef](#)]
192. Wang, X.; Zhang, C.; Zhang, Z.; Gai, Y.; Li, Q. Insights into the interfacial effects in Cu-Co/CoO catalysts on hydrogenolysis of 5-hydroxymethylfurfural to biofuel 2,5-dimethylfuran. *J. Colloid Interface Sci.* **2022**, *615*, 19–29. [[CrossRef](#)] [[PubMed](#)]
193. Yao, S.; Wang, X.; Jiang, Y.; Wu, F.; Chen, X.; Mu, X. One-step conversion of biomass-derived 5-hydroxymethylfurfural to 1,2,6-hexanetriol over Ni–Co–Al mixed oxide catalysts under mild conditions. *ACS Sustain. Chem. Eng.* **2014**, *2*, 173–180. [[CrossRef](#)]
194. Shao, Y.; Wang, J.; Sun, K.; Gao, G.; Fan, M.; Li, C.; Ming, C.; Zhang, L.; Zhang, S.; Hu, X. Cu-based nanoparticles as catalysts for selective hydrogenation of biomass-derived 5-hydroxymethylfurfural to 1,2-hexanediol. *ACS Appl. Nano Mater.* **2022**, *5*, 5882–5894. [[CrossRef](#)]
195. Li, W.; Fan, G.; Yang, L.; Li, F. Highly efficient synchronized production of phenol and 2,5-dimethylfuran through a bimetallic Ni–Cu catalyzed dehydrogenation–hydrogenation coupling process without any external hydrogen and oxygen supply. *Green Chem.* **2017**, *19*, 4353–4363. [[CrossRef](#)]
196. Xia, J.; Gao, D.; Han, F.; Li, Y.; Waterhouse, G.I.N. Efficient and selective hydrogenation of 5-hydroxymethylfurfural to 2,5-dimethylfuran over a non-noble CoNCx/NiFeO catalyst. *Catal. Lett.* **2022**, *152*, 3400–3413. [[CrossRef](#)]
197. Zhao, J.; Liu, M.; Fan, G.; Yang, L.; Li, F. Efficient transfer hydrogenolysis of 5-hydroxymethylfurfural to 2,5-dimethylfuran over cofe bimetallic catalysts using formic acid as a sustainable hydrogen donor. *Ind. Eng. Chem. Res.* **2021**, *60*, 5826–5837. [[CrossRef](#)]
198. Kataoka, H.; Kosuge, D.; Ogura, K.; Ohyama, J.; Satsuma, A. Reductive conversion of 5-hydroxymethylfurfural to 1,2,6-hexanetriol in water solvent using supported Pt catalysts. *Catal. Today* **2020**, *352*, 60–65. [[CrossRef](#)]
199. Fulignati, S.; Antonetti, C.; Licursi, D.; Pieraccioni, M.; Wilbers, E.; Heeres, H.J.; Raspolli Galletti, A.M. Insight into the hydrogenation of pure and crude HMF to furan diols using Ru/C as catalyst. *Appl. Catal. A* **2019**, *578*, 122–133. [[CrossRef](#)]
200. Farooqi, A.S.; Yusuf, M.; Zabidi, N.A.M.; Sanullah, K.; Abdullah, B. Chapter 3—CO₂ conversion technologies for clean fuels production. In *Carbon Dioxide Capture and Conversion*; Nanda, S., Vo, D.-V.N., Nguyen, V.-H., Eds.; Elsevier: Amsterdam, The Netherlands, 2022; pp. 37–63.
201. Ra, E.C.; Kim, K.Y.; Kim, E.H.; Lee, H.; An, K.; Lee, J.S. Recycling carbon dioxide through catalytic hydrogenation: Recent key developments and perspectives. *ACS Catal.* **2020**, *10*, 11318–11345. [[CrossRef](#)]
202. Fang, X.; Chen, C.; Jia, H.; Li, Y.; Liu, J.; Wang, Y.; Song, Y.; Du, T.; Liu, L. Progress in adsorption-enhanced hydrogenation of CO₂ on layered double hydroxide (LDH) derived catalysts. *J. Ind. Eng. Chem.* **2021**, *95*, 16–27. [[CrossRef](#)]
203. Álvarez, A.; Bansode, A.; Urakawa, A.; Bavykina, A.V.; Wezendonk, T.A.; Makkee, M.; Gascon, J.; Kapteijn, F. Challenges in the greener production of formates/formic acid, methanol, and dme by heterogeneously catalyzed CO₂ hydrogenation processes. *Chem. Rev.* **2017**, *117*, 9804–9838. [[CrossRef](#)] [[PubMed](#)]
204. Dewangan, N.; Hui, W.M.; Jayaprakash, S.; Bawah, A.-R.; Poerjoto, A.J.; Jie, T.; Jangam, A.; Hidajat, K.; Kawi, S. Recent progress on layered double hydroxide (ldh) derived metal-based catalysts for CO₂ conversion to valuable chemicals. *Catal. Today* **2020**, *356*, 490–513. [[CrossRef](#)]
205. Zhong, J.; Yang, X.; Wu, Z.; Liang, B.; Huang, Y.; Zhang, T. State of the art and perspectives in heterogeneous catalysis of CO₂ hydrogenation to methanol. *Chem. Soc. Rev.* **2020**, *49*, 1385–1413. [[CrossRef](#)]
206. Olah, G.A. Beyond oil and gas: The methanol economy. *Angew. Chem. Int. Ed.* **2005**, *44*, 2636–2639. [[CrossRef](#)] [[PubMed](#)]
207. Goepfert, A.; Czaun, M.; Jones, J.-P.; Surya Prakash, G.K.; Olah, G.A. Recycling of carbon dioxide to methanol and derived products—Closing the loop. *Chem. Soc. Rev.* **2014**, *43*, 7995–8048. [[CrossRef](#)]
208. Yang, M.; Fan, D.; Wei, Y.; Tian, P.; Liu, Z. Recent progress in methanol-to-olefins (mto) catalysts. *Adv. Mater.* **2019**, *31*, 1902181. [[CrossRef](#)]
209. Spencer, M.S. The role of zinc oxide in Cu/ZnO catalysts for methanol synthesis and the water–gas shift reaction. *Top. Catal.* **1999**, *8*, 259. [[CrossRef](#)]
210. Behrens, M.; Studt, F.; Kasatkin, I.; Kühl, S.; Hävecker, M.; Abild-Pedersen, F.; Zander, S.; Girgsdies, F.; Kurr, P.; Knief, B.-L.; et al. The active site of methanol synthesis over Cu/ZnO/Al₂O₃ industrial catalysts. *Science* **2012**, *336*, 893–897. [[CrossRef](#)] [[PubMed](#)]
211. Kühl, S.; Tarasov, A.; Zander, S.; Kasatkin, I.; Behrens, M. Cu-based catalyst resulting from a Cu,Zn,Al hydroxalcalite-like compound: A microstructural, thermoanalytical, and in situ xas study. *Chem.—Eur. J.* **2014**, *20*, 3782–3792. [[CrossRef](#)]
212. Gao, P.; Li, F.; Zhan, H.; Zhao, N.; Xiao, F.; Wei, W.; Zhong, L.; Wang, H.; Sun, Y. Influence of Zr on the performance of Cu/Zn/Al/Zr catalysts via hydroxalcalite-like precursors for CO₂ hydrogenation to methanol. *J. Catal.* **2013**, *298*, 51–60. [[CrossRef](#)]
213. Mureddu, M.; Lai, S.; Atzori, L.; Rombi, E.; Ferrara, F.; Pettinau, A.; Cutrufello, M.G. Ex-ldh-based catalysts for CO₂ conversion to methanol and dimethyl ether. *Catalysts* **2021**, *11*, 615. [[CrossRef](#)]

214. Gao, P.; Li, F.; Zhao, N.; Xiao, F.; Wei, W.; Zhong, L.; Sun, Y. Influence of modifier (Mn, La, Ce, Zr and Y) on the performance of Cu/Zn/Al catalysts via hydrotalcite-like precursors for CO₂ hydrogenation to methanol. *Appl. Catal. A* **2013**, *468*, 442–452. [[CrossRef](#)]
215. Gao, P.; Zhong, L.; Zhang, L.; Wang, H.; Zhao, N.; Wei, W.; Sun, Y. Yttrium oxide modified Cu/ZnO/Al₂O₃ catalysts via hydrotalcite-like precursors for CO₂ hydrogenation to methanol. *Catal. Sci. Technol.* **2015**, *5*, 4365–4377. [[CrossRef](#)]
216. Stangeland, K.; Chamssine, F.; Fu, W.; Huang, Z.; Duan, X.; Yu, Z. CO₂ hydrogenation to methanol over partially embedded cu within Zn-Al oxide and the effect of indium. *J. CO₂ Util.* **2021**, *50*, 101609. [[CrossRef](#)]
217. Zhang, F.; Liu, Y.; Xu, X.; Yang, P.; Miao, P.; Zhang, Y.; Sun, Q. Effect of al-containing precursors on Cu/ZnO/Al₂O₃ catalyst for methanol production. *Fuel Process. Technol.* **2018**, *178*, 148–155. [[CrossRef](#)]
218. Bahmani, M.; Vasheghani Farahani, B.; Sahebdehfar, S. Preparation of high performance nano-sized Cu/ZnO/Al₂O₃ methanol synthesis catalyst via aluminum hydrous oxide sol. *Appl. Catal. A* **2016**, *520*, 178–187. [[CrossRef](#)]
219. Zhao, F.; Fan, L.; Xu, K.; Hua, D.; Zhan, G.; Zhou, S.-F. Hierarchical sheet-like Cu/Zn/Al nanocatalysts derived from ldh/mof composites for CO₂ hydrogenation to methanol. *J. CO₂ Util.* **2019**, *33*, 222–232. [[CrossRef](#)]
220. Zhao, F.; Zhan, G.; Zhou, S.-F. Intercalation of laminar cu-al ldhs with molecular tcp(m) (M = Zn, Co, Ni, and Fe) towards high-performance CO₂ hydrogenation catalysts. *Nanoscale* **2020**, *12*, 13145–13156. [[CrossRef](#)]
221. Kim, J.; Jeong, C.; Baik, J.H.; Suh, Y.-W. Phases of Cu/Zn/Al/Zr precursors linked to the property and activity of their final catalysts in CO₂ hydrogenation to methanol. *Catal. Today* **2020**, *347*, 70–78. [[CrossRef](#)]
222. Frusteri, L.; Cannilla, C.; Todaro, S.; Frusteri, F.; Bonura, G. Tailoring of hydrotalcite-derived cu-based catalysts for CO₂ hydrogenation to methanol. *Catalysts* **2019**, *9*, 1058. [[CrossRef](#)]
223. Gao, P.; Li, F.; Xiao, F.; Zhao, N.; Sun, N.; Wei, W.; Zhong, L.; Sun, Y. Preparation and activity of Cu/Zn/Al/Zr catalysts via hydrotalcite-containing precursors for methanol synthesis from CO₂ hydrogenation. *Catal. Sci. Technol.* **2012**, *2*, 1447–1454. [[CrossRef](#)]
224. Gao, P.; Xie, R.; Wang, H.; Zhong, L.; Xia, L.; Zhang, Z.; Wei, W.; Sun, Y. Cu/Zn/Al/Zr catalysts via phase-pure hydrotalcite-like compounds for methanol synthesis from carbon dioxide. *J. CO₂ Util.* **2015**, *11*, 41–48. [[CrossRef](#)]
225. Gao, P.; Li, F.; Xiao, F.; Zhao, N.; Wei, W.; Zhong, L.; Sun, Y. Effect of hydrotalcite-containing precursors on the performance of Cu/Zn/Al/Zr catalysts for CO₂ hydrogenation: Introduction of Cu²⁺ at different formation stages of precursors. *Catal. Today* **2012**, *194*, 9–15. [[CrossRef](#)]
226. Zhang, F.; Zhang, Y.; Yuan, L.; Gasem, K.A.M.; Chen, J.; Chiang, F.; Wang, Y.; Fan, M. Synthesis of Cu/Zn/Al/Mg catalysts on methanol production by different precipitation methods. *Mol. Catal.* **2017**, *441*, 190–198. [[CrossRef](#)]
227. Hou, X.-X.; Xu, C.-H.; Liu, Y.-L.; Li, J.-J.; Hu, X.-D.; Liu, J.; Liu, J.-Y.; Xu, Q. Improved methanol synthesis from CO₂ hydrogenation over CuZnAlZr catalysts with precursor pre-activation by formaldehyde. *J. Catal.* **2019**, *379*, 147–153. [[CrossRef](#)]
228. Xiao, S.; Zhang, Y.; Gao, P.; Zhong, L.; Li, X.; Zhang, Z.; Wang, H.; Wei, W.; Sun, Y. Highly efficient Cu-based catalysts via hydrotalcite-like precursors for CO₂ hydrogenation to methanol. *Catal. Today* **2017**, *281*, 327–336. [[CrossRef](#)]
229. Zhang, C.; Yang, H.; Gao, P.; Zhu, H.; Zhong, L.; Wang, H.; Wei, W.; Sun, Y. Preparation and CO₂ hydrogenation catalytic properties of alumina microsphere supported cu-based catalyst by deposition-precipitation method. *J. CO₂ Util.* **2017**, *17*, 263–272. [[CrossRef](#)]
230. Kattel, S.; Ramírez, P.J.; Chen, J.G.; Rodriguez, J.A.; Liu, P. Active sites for CO₂ hydrogenation to methanol on Cu/ZnO catalysts. *Science* **2017**, *355*, 1296–1299. [[CrossRef](#)]
231. Kurtz, M.; Wilmer, H.; Genger, T.; Hinrichsen, O.; Muhler, M. Deactivation of supported copper catalysts for methanol synthesis. *Catal. Lett.* **2003**, *86*, 77–80. [[CrossRef](#)]
232. Kühl, S.; Schumann, J.; Kasatkin, I.; Hävecker, M.; Schlögl, R.; Behrens, M. Ternary and quaternary Cr or Ga-containing ex-ldh catalysts—Influence of the additional oxides onto the microstructure and activity of Cu/ZnAl₂O₄ catalysts. *Catal. Today* **2015**, *246*, 92–100. [[CrossRef](#)]
233. Li, M.M.J.; Chen, C.; Ayvalı, T.; Suo, H.; Zheng, J.; Teixeira, I.F.; Ye, L.; Zou, H.; O'Hare, D.; Tsang, S.C.E. CO₂ hydrogenation to methanol over catalysts derived from single cationic layer CuZnGa LDH precursors. *ACS Catal.* **2018**, *8*, 4390–4401. [[CrossRef](#)]
234. Zheng, H.; Narkhede, N.; Zhang, G.; Zhang, H.; Ma, L.; Yu, S. Highly dispersed cu catalyst based on the layer confinement effect of Cu/Zn/Ga-ldh for methanol synthesis. *Mol. Catal.* **2021**, *516*, 111984. [[CrossRef](#)]
235. Younas, M.; Loong Kong, L.; Bashir, M.J.K.; Nadeem, H.; Shehzad, A.; Sethupathi, S. Recent advancements, fundamental challenges, and opportunities in catalytic methanation of CO₂. *Energy Fuels* **2016**, *30*, 8815–8831. [[CrossRef](#)]
236. Wei, W.; Jinlong, G. Methanation of carbon dioxide: An overview. *Front. Chem. Sci. Eng.* **2011**, *5*, 2–10. [[CrossRef](#)]
237. Guo, X.; Peng, Z.; Hu, M.; Zuo, C.; Traitangwong, A.; Meeyoo, V.; Li, C.; Zhang, S. Highly active Ni-based catalyst derived from double hydroxides precursor for low temperature CO₂ methanation. *Ind. Eng. Chem. Res.* **2018**, *57*, 9102–9111. [[CrossRef](#)]
238. Pan, Q.; Peng, J.; Sun, T.; Wang, S.; Wang, S. Insight into the reaction route of CO₂ methanation: Promotion effect of medium basic sites. *Catal. Commun.* **2014**, *45*, 74–78. [[CrossRef](#)]
239. He, L.; Lin, Q.; Liu, Y.; Huang, Y. Unique catalysis of ni-al hydrotalcite derived catalyst in CO₂ methanation: Cooperative effect between ni nanoparticles and a basic support. *J. Energy Chem.* **2014**, *23*, 587–592. [[CrossRef](#)]
240. Sun, C.; Świrk, K.; Wierzbicki, D.; Motak, M.; Grzybek, T.; Da Costa, P. On the effect of yttrium promotion on ni-layered double hydroxides-derived catalysts for hydrogenation of CO₂ to methane. *Int. J. Hydrogen Energy* **2021**, *46*, 12169–12179. [[CrossRef](#)]

241. Summa, P.; Samojeden, B.; Motak, M.; Wierzbicki, D.; Alxneit, I.; Świerczek, K.; Da Costa, P. Investigation of Cu promotion effect on hydrotalcite-based nickel catalyst for CO₂ methanation. *Catal. Today* **2022**, *384*, 133–145. [[CrossRef](#)]
242. Xiao, X.; Wang, J.; Li, J.; Dai, H.; Jing, F.; Liu, Y.; Chu, W. Enhanced low-temperature catalytic performance in CO₂ hydrogenation over Mn-promoted NiMgAl catalysts derived from quaternary hydrotalcite-like compounds. *Int. J. Hydrogen Energy* **2021**, *46*, 33107–33119. [[CrossRef](#)]
243. Aldana, P.A.U.; Ocampo, F.; Kobl, K.; Louis, B.; Thibault-Starzyk, F.; Daturi, M.; Bazin, P.; Thomas, S.; Roger, A.C. Catalytic CO₂ valorization into CH₄ on Ni-based ceria-zirconia. Reaction mechanism by operando Ir spectroscopy. *Catal. Today* **2013**, *215*, 201–207. [[CrossRef](#)]
244. Liu, J.; Bing, W.; Xue, X.; Wang, F.; Wang, B.; He, S.; Zhang, Y.; Wei, M. Alkaline-assisted Ni nanocatalysts with largely enhanced low-temperature activity toward CO₂ methanation. *Catal. Sci. Technol.* **2016**, *6*, 3976–3983. [[CrossRef](#)]
245. Guo, X.; Gao, D.; He, H.; Traitangwong, A.; Gong, M.; Meeyoo, V.; Peng, Z.; Li, C. Promotion of CO₂ methanation at low temperature over hydrotalcite-derived catalysts—effect of the tunable metal species and basicity. *Int. J. Hydrogen Energy* **2021**, *46*, 518–530. [[CrossRef](#)]
246. Yin, L.; Chen, X.; Sun, M.; Zhao, B.; Chen, J.; Zhang, Q.; Ning, P. Insight into the role of Fe on catalytic performance over the hydrotalcite-derived Ni-based catalysts for CO₂ methanation reaction. *Int. J. Hydrogen Energy* **2022**, *47*, 7139–7149. [[CrossRef](#)]
247. Świrk, K.; Summa, P.; Wierzbicki, D.; Motak, M.; Da Costa, P. Vanadium promoted Ni(Mg,Al)O hydrotalcite-derived catalysts for CO₂ methanation. *Int. J. Hydrogen Energy* **2021**, *46*, 17776–17783. [[CrossRef](#)]
248. Mebrahtu, C.; Krebs, F.; Perathoner, S.; Abate, S.; Centi, G.; Palkovits, R. Hydrotalcite based Ni–Fe/(Mg, Al)O_x catalysts for CO₂ methanation—Tailoring Fe content for improved CO dissociation, basicity, and particle size. *Catal. Sci. Technol.* **2018**, *8*, 1016–1027. [[CrossRef](#)]
249. He, F.; Zhuang, J.; Lu, B.; Liu, X.; Zhang, J.; Gu, F.; Zhu, M.; Xu, J.; Zhong, Z.; Xu, G.; et al. Ni-based catalysts derived from Ni-Zr-Al ternary hydrotalcites show outstanding catalytic properties for low-temperature CO₂ methanation. *Appl. Catal. B* **2021**, *293*, 120218. [[CrossRef](#)]
250. Zhang, Q.; Xu, R.; Liu, N.; Dai, C.; Yu, G.; Wang, N.; Chen, B. In Situ Ce-doped catalyst derived from NiCeAl-ldhs with enhanced low-temperature performance for CO₂ methanation. *Appl. Surf. Sci.* **2022**, *579*, 152204. [[CrossRef](#)]
251. Lee, W.J.; Li, C.; Prajitno, H.; Yoo, J.; Patel, J.; Yang, Y.; Lim, S. Recent trend in thermal catalytic low temperature CO₂ methanation: A critical review. *Catal. Today* **2021**, *368*, 2–19. [[CrossRef](#)]
252. Zhang, L.; Bian, L.; Zhu, Z.; Li, Z. La-promoted Ni/Mg-Al catalysts with highly enhanced low-temperature CO₂ methanation performance. *Int. J. Hydrogen Energy* **2018**, *43*, 2197–2206. [[CrossRef](#)]
253. Ho, P.H.; de Luna, G.S.; Angelucci, S.; Canciani, A.; Jones, W.; Decarolis, D.; Ospitali, F.; Aguado, E.R.; Rodríguez-Castellón, E.; Fornasari, G.; et al. Understanding structure-activity relationships in highly active La promoted Ni catalysts for CO₂ methanation. *Appl. Catal. B* **2020**, *278*, 119256. [[CrossRef](#)]
254. Jiang, F.; Wang, S.; Liu, B.; Liu, J.; Wang, L.; Xiao, Y.; Xu, Y.; Liu, X. Insights into the influence of CeO₂ crystal facet on CO₂ hydrogenation to methanol over Pd/CeO₂ catalysts. *ACS Catal.* **2020**, *10*, 11493–11509. [[CrossRef](#)]
255. Guo, X.; He, H.; Traitangwong, A.; Gong, M.; Meeyoo, V.; Li, P.; Li, C.; Peng, Z.; Zhang, S. Ceria imparts superior low temperature activity to nickel catalysts for CO₂ methanation. *Catal. Sci. Technol.* **2019**, *9*, 5636–5650. [[CrossRef](#)]
256. Malkar, R.S.; Yadav, G.D. Selectivity engineering in one pot synthesis of raspberry ketone: Crossed aldol condensation of p-hydroxybenzaldehyde and acetone and hydrogenation over novel Ni/Zn-La mixed oxide. *ChemistrySelect* **2019**, *4*, 2140–2152. [[CrossRef](#)]
257. Novodárszki, G.; Onyestyák, G.; Barthos, R.; Wellisch, Á.F.; Thakur, A.J.; Deka, D.; Valyon, J. Guerbet alkylation of acetone by ethanol and reduction of product alkylate to alkane over tandem nickel/Mg,Al-hydrotalcite and nickel molybdate/ γ -alumina catalyst systems. *React. Kinet. Mech. Catal.* **2017**, *121*, 69–81. [[CrossRef](#)]
258. Fridrich, B.; Stuart, M.C.A.; Barta, K. Selective coupling of bioderived aliphatic alcohols with acetone using hydrotalcite derived Mg–Al porous metal oxide and Raney nickel. *ACS Sustain. Chem. Eng.* **2018**, *6*, 8468–8475. [[CrossRef](#)]
259. Onyestyák, G.; Novodárszki, G.; Farkas Wellisch, Á.; Pilbáth, A. Upgraded biofuel from alcohol–acetone feedstocks over a two-stage flow-through catalytic system. *Catal. Sci. Technol.* **2016**, *6*, 4516–4524. [[CrossRef](#)]
260. Ramos, R.; Tišler, Z.; Kikhtyanin, O.; Kubička, D. Towards understanding the hydrodeoxygenation pathways of furfural–acetone aldol condensation products over supported Pt catalysts. *Catal. Sci. Technol.* **2016**, *6*, 1829–1841. [[CrossRef](#)]
261. Yang, J.; Li, S.; Li, N.; Wang, W.; Wang, A.; Zhang, T.; Cong, Y.; Wang, X.; Huber, G.W. Synthesis of jet-fuel range cycloalkanes from the mixtures of cyclopentanone and butanal. *Ind. Eng. Chem. Res.* **2015**, *54*, 11825–11837. [[CrossRef](#)]
262. Onyestyák, G.; Novodárszki, G.; Barthos, R.; Klébert, S.; Wellisch, Á.F.; Pilbáth, A. Acetone alkylation with ethanol over multifunctional catalysts by a borrowing hydrogen strategy. *RSC Adv.* **2015**, *5*, 99502–99509. [[CrossRef](#)]
263. Al-Wadaani, F.; Kozhevnikova, E.F.; Kozhevnikov, I.V. Pd supported on ZnII–CrIII mixed oxide as a catalyst for one-step synthesis of methyl isobutyl ketone. *J. Catal.* **2008**, *257*, 199–205. [[CrossRef](#)]
264. Nikolopoulos, A.A.; Jang, B.W.L.; Spivey, J.J. Acetone condensation and selective hydrogenation to MIBK on Pd and Pt hydrotalcite-derived Mg–Al mixed oxide catalysts. *Appl. Catal. A* **2005**, *296*, 128–136. [[CrossRef](#)]
265. Das, N.N.; Das, R. Synthesis, characterization and activation of quaternary layered double hydroxides for the one-pot synthesis of methyl isobutyl ketone. *React. Kinet. Mech. Catal.* **2010**, *99*, 397–408. [[CrossRef](#)]

266. Hetterley, R.D.; Mackey, R.; Jones, J.T.A.; Khimiyak, Y.Z.; Fogg, A.M.; Kozhevnikov, I.V. One-step conversion of acetone to methyl isobutyl ketone over pd-mixed oxide catalysts prepared from novel layered double hydroxides. *J. Catal.* **2008**, *258*, 250–255. [[CrossRef](#)]
267. Shen, Y.; Yi, J.; Yan, Y.; Liu, D.; Fan, L.; Li, S. Hydrogenation and condensation of acetone over Ni/MgO–Al₂O₃ prepared from hydrotalcite precursors. *J. Chem. Eng. Jpn.* **2016**, *49*, 656–662. [[CrossRef](#)]
268. Basu, S.; Sarkar, J.J.; Pradhan, N.C. Selective synthesis of MIBK via acetone hydrogenation over Cu–Al mixed oxide catalysts. *Catal. Today* **2021**, *404*, 182–189. [[CrossRef](#)]
269. Li, X.; Sun, J.; Shao, S.; Hu, X.; Cai, Y. Aldol condensation/hydrogenation for jet fuel from biomass-derived ketone platform compound in one pot. *Fuel Process. Technol.* **2021**, *215*, 106768. [[CrossRef](#)]
270. Shao, S.; Hu, X.; Dong, W.; Li, X.; Zhang, H.; Xiao, R.; Cai, Y. Integrated C–C coupling/hydrogenation of ketones derived from biomass pyrolysis for aviation fuel over Ni/Mg–Al–O/Ac bifunctional catalysts. *J. Clean. Prod.* **2021**, *282*, 124331. [[CrossRef](#)]
271. Sheng, X.; Li, G.; Wang, W.; Cong, Y.; Wang, X.; Huber, G.W.; Li, N.; Wang, A.; Zhang, T. Dual-bed catalyst system for the direct synthesis of high density aviation fuel with cyclopentanone from lignocellulose. *AIChE J.* **2016**, *62*, 2754–2761. [[CrossRef](#)]
272. Sheng, X.; Li, N.; Li, G.; Wang, W.; Wang, A.; Cong, Y.; Wang, X.; Zhang, T. Direct synthesis of renewable dodecanol and dodecane with methyl isobutyl ketone over dual-bed catalyst systems. *ChemSusChem* **2017**, *10*, 825–829. [[CrossRef](#)]
273. Luggren, P.J.; Apestequiá, C.R.; Di Cosimo, J.I. Upgrading of biomass-derived 2-hexanol to liquid transportation fuels on Cu–Mg–Al mixed oxides. Effect of Cu content. *Fuel* **2016**, *177*, 28–38. [[CrossRef](#)]
274. Zhong, Y.; Zhou, B.; Wang, L. Fe/FeO_x embedded in LDH catalyzing C–C bond forming reactions of furfural with alcohols in the absence of a homogeneous base. *Mol. Catal.* **2020**, *493*, 111056. [[CrossRef](#)]
275. Hernández, W.Y.; De Vlieger, K.; Van Der Voort, P.; Verberckmoes, A. Ni–Cu hydrotalcite-derived mixed oxides as highly selective and stable catalysts for the synthesis of β -branched bioalcohols by the guerbet reaction. *ChemSusChem* **2016**, *9*, 3196–3205. [[CrossRef](#)] [[PubMed](#)]
276. Li, J.; Lin, L.; Tan, Y.; Wang, S.; Yang, W.; Chen, X.; Luo, W.; Ding, Y.-J. High performing and stable Cu/NiAlO_x catalysts for the continuous catalytic conversion of ethanol into butanol. *ChemCatChem* **2022**, *14*, e202200539.
277. Pang, J.; Zheng, M.; He, L.; Li, L.; Pan, X.; Wang, A.; Wang, X.; Zhang, T. Upgrading ethanol to n-butanol over highly dispersed Ni–MgAlO catalysts. *J. Catal.* **2016**, *344*, 184–193. [[CrossRef](#)]
278. Song, J.; Huang, Z.-F.; Pan, L.; Li, K.; Zhang, X.; Wang, L.; Zou, J.-J. Review on selective hydrogenation of nitroarene by catalytic, photocatalytic and electrocatalytic reactions. *Appl. Catal. B* **2018**, *227*, 386–408. [[CrossRef](#)]
279. Wang, J.; Du, C.; Wei, Q.; Shen, W. Two-dimensional pd nanosheets with enhanced catalytic activity for selective hydrogenation of nitrobenzene to aniline. *Energy Fuels* **2021**, *35*, 4358–4366. [[CrossRef](#)]
280. Kowalewski, E.; Krawczyk, M.; Słowik, G.; Kocik, J.; Pieta, I.S.; Chernyayeva, O.; Lisovytskiy, D.; Matus, K.; Śrębowata, A. Continuous-flow hydrogenation of nitrocyclohexane toward value-added products with CuZnAl hydrotalcite derived materials. *Appl. Catal. A* **2021**, *618*, 118134. [[CrossRef](#)]
281. Corma, A.; Serna, P. Chemoselective hydrogenation of nitro compounds with supported gold catalysts. *Science* **2006**, *313*, 332–334. [[CrossRef](#)]
282. Tan, Y.; Liu, X.Y.; Zhang, L.; Wang, A.; Li, L.; Pan, X.; Miao, S.; Haruta, M.; Wei, H.; Wang, H. ZnAl-hydrotalcite-supported Au₂₅ nanoclusters as precatalysts for chemoselective hydrogenation of 3-nitrostyrene. *Angew. Chem.* **2017**, *129*, 2753–2757. [[CrossRef](#)]
283. Tan, Y.; Liu, X.Y.; Li, L.; Kang, L.; Wang, A.; Zhang, T. Effects of divalent metal ions of hydrotalcites on catalytic behavior of supported gold nanocatalysts for chemoselective hydrogenation of 3-nitrostyrene. *J. Catal.* **2018**, *364*, 174–182. [[CrossRef](#)]
284. Zhao, J.; Yuan, H.; Li, J.; Bing, W.; Yang, W.; Liu, Y.; Chen, J.; Wei, C.; Zhou, L.; Fang, S. Effects of preparation parameters of nial oxide-supported Au catalysts on nitro compounds chemoselective hydrogenation. *ACS Omega* **2020**, *5*, 7011–7017. [[CrossRef](#)]
285. Lu, Q.; Liu, J.; Ma, L. Recent advances in selective catalytic hydrogenation of nitriles to primary amines. *J. Catal.* **2021**, *404*, 475–492. [[CrossRef](#)]
286. Tichit, D.; Medina, F.; Durand, R.; Mateo, C.; Coq, B.; Sueiras, J.E.; Salagre, P. Use of ni containing anionic clay minerals as precursors of catalysts for the hydrogenation of nitriles. In *Studies in Surface Science and Catalysis*; Blaser, H.U., Baiker, A., Prins, R., Eds.; Elsevier: Amsterdam, The Netherlands, 1997; Volume 108, pp. 297–304.
287. Coq, B.; Tichit, D.; Ribet, S. Co/Ni/Mg/Al layered double hydroxides as precursors of catalysts for the hydrogenation of nitriles: Hydrogenation of acetonitrile. *J. Catal.* **2000**, *189*, 117–128. [[CrossRef](#)]
288. Cao, Y.; Niu, L.; Wen, X.; Feng, W.; Huo, L.; Bai, G. Novel layered double hydroxide/oxide-coated nickel-based core–shell nanocomposites for benzonitrile selective hydrogenation: An interesting water switch. *J. Catal.* **2016**, *339*, 9–13. [[CrossRef](#)]
289. Cao, Y.; Zhang, H.; Dong, J.; Ma, Y.; Sun, H.; Niu, L.; Lan, X.; Cao, L.; Bai, G. A stable nickel-based catalyst derived from layered double hydroxide for selective hydrogenation of benzonitrile. *Mol. Catal.* **2019**, *475*, 110452. [[CrossRef](#)]
290. Sheng, M.; Yamaguchi, S.; Nakata, A.; Yamazoe, S.; Nakajima, K.; Yamasaki, J.; Mizugaki, T.; Mitsudome, T. Hydrotalcite-supported cobalt phosphide nanorods as a highly active and reusable heterogeneous catalyst for ammonia-free selective hydrogenation of nitriles to primary amines. *ACS Sustain. Chem. Eng.* **2021**, *9*, 11238–11246. [[CrossRef](#)]